The Development of 3D Metamaterials with Independent and Controllable Electric and Magnetic Properties

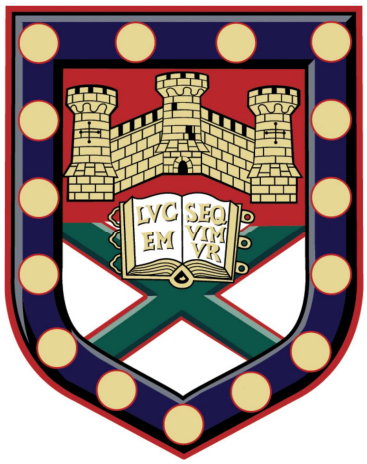

Toby Ian Campbell
School of Physics
University of Exeter

A thesis submitted for the degree of
Master of Philosophy in Physics
January 2013

The Development of 3D Metamaterials with Independent and Controllable Electric and Magnetic Properties

Submitted by Toby Ian Campbell to the University of Exeter as a thesis for the degree of Master of Philosophy in Physics
January 2013

I certify that all material in this thesis which is not my own work has been identified and that no material has previously been submitted and approved for the award of a degree by this or any other University.

Toby Campbell
January 2013

Abstract

The work detailed within this thesis concerns the development of 3D metamaterials with independent and controllable electric and magnetic properties over a large frequency range.

Electromagnetic (EM) responses of 3D metamaterial structures are investigated and the effect of changing the shape of individual elements that make up the structure is explored. A novel broad-band metamaterial structure comprising an array of cubic elements made of cross-linked flat metal plates has been fabricated and characterised using a stripline technique. Forming a slab of metamaterial from a set of subunits has allowed the transmission and reflection characteristics to be obtained, from which the effective electromagnetic parameters of the metamaterial have been extracted. Results correlate well with finite element field simulations and show that by changing the structure of the individual elements it is possible to suitably increase the effective refractive index of the structure. The individual elements are changed so that capacitive effects between neighbouring elements, which dictates the permittivity, is maintained while the area subtended by the current loops, which dictates the permeability, is reduced. EM modelling of such structures also demonstrates that the electric and magnetic fields are decomposed into different regions of the structure.

EM modelling is used to investigate more elaborate metamaterial structures, where the field decomposition is exploited by filling different regions of the structure with ‘naturally’ high permittivity and permeability materials. Filling the structure gives further independent control of the electric and magnetic properties of the structured material. Varying the amount and type of spacer material between elements is also shown to introduce anisotropy into the structure.

Table of Contents

List of Figures

Acknowledgements

Undertaking a part time MPhil at the University of Exeter while living and working in Preston has at times been challenging but I have had many people to help me along the way. First and foremost I want to thank my supervisors Roy Sambles and Alastair Hibbins. Their enthusiasm for the subject is a real inspiration. Although, through my day job at BAE Systems, I have attained a good engineering level understanding of Electromagnetics, Roy and Alastair have really given me an insight into the underlying fundamental physics that governs how electromagnetic waves interact with materials and structures. As well as help from Roy and Alastair I have had much help and support from the whole of the University of Exeter Electromagnetic and Acoustic Materials Group. In particular Ian Hooper's help with the stripline measurements and his work constructing a fitting routine for the extraction of the permittivity and permeability of a material has been invaluable and very much appreciated. I would also like to thank Alex Patterson and Ruth Lovelock, two summer students who worked within the Electromagnetics Materials group and helped me with sample fabrication and the preliminary material characterisation measurements.

In addition to the support from University of Exeter I also had much support from my colleagues at BAE Systems. In particular I would like to thank Stewart Wylie, Ian MacDiarmid and Sajad Haq for their technical advice and guidance and to my managers Nigel Wignall and Graham Roebuck for their understanding and flexible approach allowing me to take time out from my day job to visit Exeter and work on my MPhil.

Lastly I would like to thank my family and friends for their love and encouragement. For my parents who are always supportive and also provided me with a place to stay on my frequent visits to the southwest. And most of all to my loving and supportive girlfriend Amy whose faithful support during the final stages of my MPhil is so appreciated. Thank you.

1 Introduction and Review

The work detailed within this thesis concerns the development of 3D metamaterials with independent and controllable electric and magnetic properties over a large frequency range.

In most magnetic composite materials there is an inherent link between the permittivity and permeability of the material. There are many applications where breaking this link and having more independent control of the electric and magnetic properties of the material would be highly beneficial. Work detailed in this thesis explores the possibility of using a 3D structured metamaterial to give a higher level of independence between the effective electric and magnetic properties.

1.1 Introduction

This chapter introduces the concept of electromagnetic metamaterials and reviews some of the work carried out within this vast field of research including a brief overview of the historical origins of this area of research. The area of transformation optics is introduced, which is a tool for designing novel electromagnetic structures and provides useful context as to why controlling the electric and magnetic properties of a material is so important. The main body of the review concerns the development of metallic based metamaterials, from arrays of thin wires through to more elaborate arrays of 3D elements.

Shin et al. [1] proposed, in 2009, that 3D metamaterial structures could be used to achieve a broadband, high index material. The structure can be considered a metamaterial since the period of the array is much smaller than the wavelengths of interest. The metamaterial consists of a periodic array of cubic elements where the size, spacing, structure and material of the elements dictate the electromagnetic response. In this thesis, we experimentally explore the electromagnetic response of structures similar to that theoretically proposed by Shin et al. A more detailed description of the structures explored is given later

in this thesis, but for visualisation purposes the simplest structure consisting of regular, perfectly electrically conducting (PEC) cubes is shown in Figure 1.

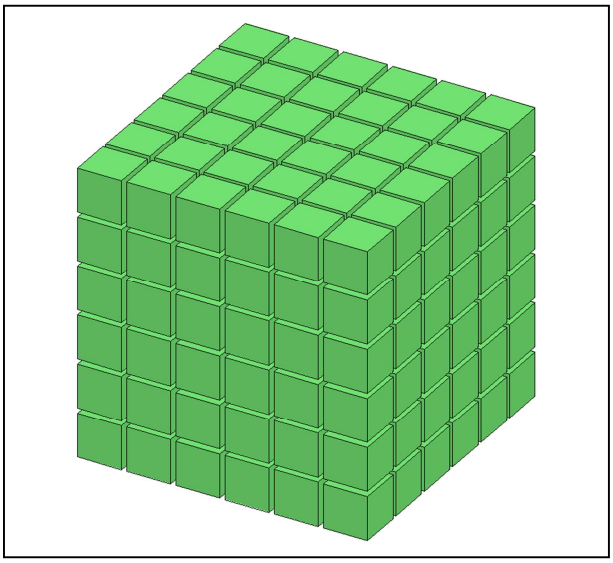

Figure 1: An illustration of the simplest cubic array structure studied, consisting of PEC cubic elements.

Shin et al. vary the structure of the cubic metal elements, reducing the area of the current loops in the individual elements, which control the magnetic properties, whilst maintaining a strong capacitive effect between elements, which determines electric properties. Shin et al show that the refractive index can be maintained at arbitrarily high values by using a periodic structure of isolated elements. These consist of connected, structured plates which allow control of the effective permittivity and permeability without the use of resonant and inherently narrow-band structures.

Chapter 2 details the electromagnetic modelling and measurement methods used to investigate the electromagnetic characteristics of the structures studied within this thesis. Finite element modelling techniques are applied to the simplest array of solid metal cubes with the transmission responses, field plots and extracted constitutive parameters being used to explore the effect of changing the key parameters. Chapter 2 also details the experimental methods, including sample fabrication, and the measurement techniques as well as showing a typical transmission response and detailing the methods used for extracting the effective permittivity and permeability.

Chapter 3 reports the experimental measurement from of a number of structures. Extensive discussion of the results and extracted parameters is presented and FEM modelled responses as well as field plots are generated to explain the behaviour seen.

The decomposition of the electric and magnetic fields into different regions of the structure is exploited and detailed in Chapter 4. Filling different regions of the structure with conventional materials with higher permittivity and permeability than air further increases the independent control of the electric and magnetic properties. The introduction of anisotropy into the structure by varying element spacing is also investigated.

Finally, Chapter 5 summarises the findings of the work detailed within this thesis and discusses areas of possible future work.

1.2 Electromagnetic Metamaterials Review

The electromagnetic response of materials is dependent on their microscopic make-up and is described by their constitutive parameters; the permittivity ε and the permeability μ. Metamaterials are synthetic engineered electromagnetic composites which give designer-controlled constitutive parameters by virtue of structure. We return to the development of metallic based metamaterials later in this review; however we first consider the area of metamaterials known as transformation optics as it provides a useful context to the work detailed in this thesis.

1.2.1 Transformation Optics

In 2006 both Pendry and colleagues and Leonhardt introduced the concept of transformation optics [2] [3]. In Pendry and colleague's paper it states (the fairly obvious) that materials can be used to control and direct electromagnetic fields. Metamaterials are introduced and it is assumed that a material can be constructed where the permittivity and permeability values may be designed to vary independently and arbitrarily throughout a material. We return to this assumption later in this chapter. Pendry et al. outline an approach to defining

the ‘recipe’ of desired properties for metamaterials using coordinate transformations. An example is given of a uniform field expressed on a Cartesian mesh which is pulled and stretched. Distortion can be recorded as a coordinate transform between the original Cartesian mesh and the distorted mesh. When the new coordinate system is substituted, Maxwell’s equations maintain the same form, but the permittivity and permeability are scaled by a common factor. This then gives a recipe for how permittivity and permeability are required to vary within the material in order to achieve the change in fields required. This approach is used to demonstrate a cloak in which a device is concealed with incoming radiation being simply guided by the cloak around the object to emerge travelling in the same direction as if it had passed through an empty volume of space.

The 2006 papers by Pendry et al. and Leonhardt gave rise to the area of transformation optics, which is being used extensively to explore possible novel electromagnetic structures which then require new metamaterials with defined properties, sometimes with negative index for example.

One example of how transformation optics can be used is the exploration of reflectionless media by Rahm et al. [4]. Embedded coordinate transforms are used which adds flexibility to the transformation optics approach by enabling the transfer of field manipulation from one material to another. Transformation equations are defined for confined regions of space from which a tensor describing the relative permittivity and permeability can be calculated. Coordinate transforms are calculated for reflectionless beam shifters and beam splitters which result in a required relative permittivity and permeability of the form

$$\varepsilon_r^{ij} = \mu_r^{ij} = \frac{1}{a_{22}} g^{ij}$$

where g^{ij} is the metric tensor of the coordinate transform and a determines the shift amount. It is shown that reflectionless beam shifters and beam splitters require an anisotropic material with spatially varying permittivity and

permeability. For these reflectionless media a negative index material is not an essential requirement. Figure 2 shows a 2D full wave simulation of a beam splitting device.

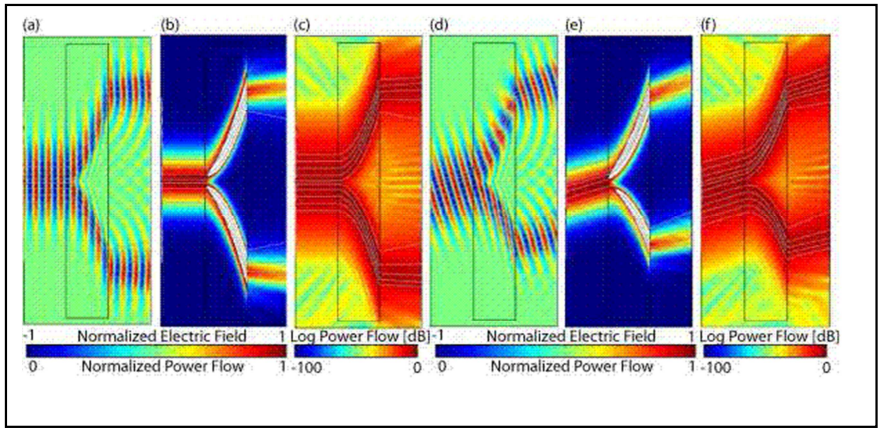

Figure 2: Electric field distribution (colour map) [(a) and (d)] and power flow [(b), (c), (e) and (f)] of a beam splitter for diffracting plane waves for perpendicular (a-c) and oblique incidence(d-f). Figure extracted directly from [4].

Transformation optics has now been considered for a wide range of applications such as cloaking structures [5] [6], flat lenses [7] and antennas [8] [9]. Using transformational optics Tichit et al. [8] define the permittivity and permeability tensors of the metamaterial designed to transform an isotropically radiating source into a compact highly directive antenna. It is shown that the directivity of the metamaterial antenna is comparable to conventional directive antennas (horn and reflector antenna) with the overall dimensions of the antenna being reduced.

Transformation optics provides an elegant method for generating the 'recipe' for permittivity and permeability for a wide range of potential metamaterial applications. Two of the key elements of the material 'recipe' prescribed by transformation optics are for materials to have a controllable positive index and for the material to be anisotropic. The work detailed in this thesis goes some way to providing metamaterials with these two key characteristics.

1.2.2 Metallic Metamaterials

The main area of metamaterials research concerns creating materials with exotic electric and magnetic properties.

In the first half of the 20th century artificial materials that manipulated electromagnetic waves were investigated by the likes of Bose [10], Lindell et al. [11] and Kock [12]. Materials investigated include chiral and conductive elements arranged periodically in host media. Artificial materials were further developed over the remainder of the 20th century as materials, manufacturing and fabrication techniques matured.

In 1967 Vesalago theoretically investigated plane waves interacting with an imaginary material with a negative permittivity and permeability and proposed the concept of negative (unnatural) refraction [13]. In the 1990s Pendry et al. investigated periodic thin wire and split ring structures. The label metamaterials was introduced, and in 1999 Pendry et al. published their seminal paper [14] proposing a negative index material. This is widely acknowledged as the beginning of the modern research area known as metamaterials. It should be noted that although this thesis is not concerned with negative index materials it is appropriate to mention them here due to their importance in the expansion of the metamaterials field of research.

In the 1990's Pendry et al. began to investigate periodic metallic structures with a unit cell of characteristic dimension, a, for which the contents of the unit cell define the effective response of the system as a whole. Permittivity and permeability had previously been used to present a homogenous view of the electromagnetic properties of a medium, but it was shown that an effective permittivity and permeability concept was valid for such a metamaterial provided that $a << \lambda$, where λ is the wavelength **within** the medium.

The first periodic structure to be investigated consisted of very thin wires arranged in a 3D lattice [14] which was shown to have negative permittivity. Other structures such as arrays of non-magnetic metallic cylinders, coils and split ring resonators were investigated and shown to respond to microwave radiation with an effective permittivity and permeability controlled by the structure [14] [15]. A wide range of effective electromagnetic properties were achieved, beyond that found in nature, by varying the parameters of the unit cell [16].

Although negative index materials still formed the focus of much metamaterials research there was also work being carried out investigating other broader-band metamaterials such as high impedance surfaces [17] [18], broadband absorbers [19, 20], artificial magnetic conductors [21] [22] and high index materials [1] [23].

One example of a broadband structure being investigated was a 2D array consisting of metal films with periodic arrangements of cut-through slits. It was shown by Shen et al. [23] that a perfect metal sheet with periodic slits can be regarded as a dielectric slab with a frequency independent refractive index with the index of the 2D array shown to be entirely controlled by the geometry of the structure. It was shown that the existence of a propagating transverse electromagnetic (TEM) mode in a sub-wavelength slit allows perfect transmission through the array with the electric properties of the metal film array, in the long wavelength limit, asymptotically approaching that of an equivalent dielectric slab. The frequency dependent refractive index of the two-dimensional array is entirely controlled by the geometry of the structure.

Theoretical work on 2D arrays was then extended to three dimensions by Wood and Pendry [24] examining the response of metamaterials at zero frequency. With an expressed aim of producing a metamaterial suitable for cloaking an object from a DC magnetic field, Wood and Pendry stated that a diamagnetic material with a high degree of anisotropy was required. To this end, three dimensional structures consisting of superconducting elements were investigated. A three dimensional array of cubes was first investigated [24] and it was shown that as the cube size *d* approaches the lattice constant *l* then a good estimate of the permittivity and permeability can be obtained,

$$\boldsymbol{\varepsilon_{eff}} = \frac{\boldsymbol{d^2}}{\boldsymbol{l(l-d)}} \qquad \boldsymbol{\mu_{eff}} = \frac{\boldsymbol{l^2-d^2}}{\boldsymbol{l^2}}. \tag{1}$$

This result will be used to corroborate EM modelling carried out for such structures in Chapter 2.

More complicated structures consisting of flattened plates [24] in various configurations giving differing levels of anisotropy were investigated and the analytical method extended to characterise structures such as those shown in Figure 3.

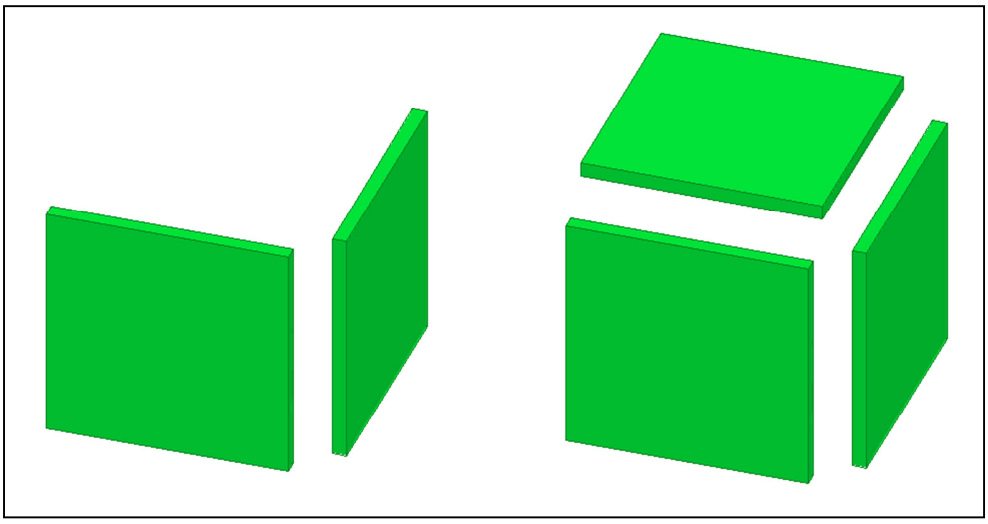

Figure 3: Unit cell structures for a 2-plate and 3-plate array of cubic elements.

The ideas explored by Shen et al. and Wood were brought together by Shin et al. [1] who proposed a broadband metamaterial that has an enhanced refractive index through the use of a three dimensional array with elements constructed of suitably connected metal plates. Previous work showed that a sub-wavelength array of parallel plate capacitors could lead to broadband enhancement of permittivity [23] [25]. These structures however exhibited strong diamagnetic effects i.e. a suppressed permeability. The work of Shin et al. is primarily concerned with avoiding this effect, exploring a general mechanism for enhancing the permittivity by generating a large electric dipole response while maintaining permeability through the prevention of the formation of large area current loops.

Shin's paper and much of the work detailed in this thesis concerns structures made up from cubic structured elements such as illustrated in Figure 4.

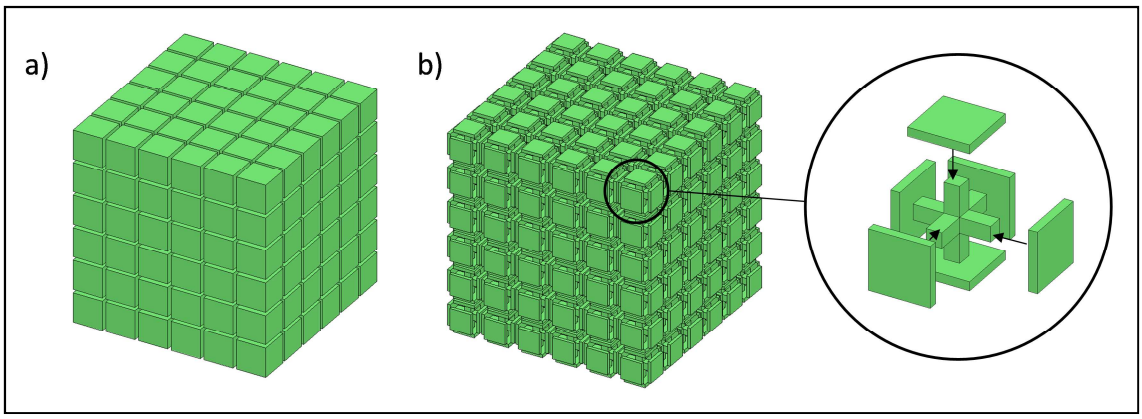

Figure 4: Illustration of a) an array of cubes and b) an array of structured elements.

An array of cubes was first considered consisting of perfectly electrically conducting (PEC) cubes suspended in air. The model response of this structure to incident microwaves shows that the permittivity is determined by the capacitive effects between neighbouring cubes while the permeability is governed by the current loops around the cubes. A key observation highlighted was that the permittivity, ε, and permeability, μ, are controlled by different aspects of the structure. Higher index structures were proposed which suppress the diamagnetic response by reducing the loop area while maintaining a strong capacitive response. This was achieved by replacing each cube with an element consisting of six metal plates connected by three orthogonal metal wires intersecting at the centre of the unit cell. This structure maintained the capacitive elements of the cubes while reducing the area of the current loops. A key feature is that the electric and magnetic fields are decomposed with the electric field concentrated in the area between the plates of neighbouring elements while being excluded from the internal area of the element. This resulted in ε being maintained while μ increases, thereby increasing the bulk refractive index of the structured material and allowing the impedance to be controlled independently of the index. Shin et al. [1] show that these structures could give an extremely high effective refractive index enhancement. (It should be noted that while these broadband structures were proposed theoretically, they were not experimentally validated).

Shin et al [1] demonstrated theoretically that the diamagnetic response could be reduced further through appropriate structuring of the plates of the capacitor array, and proposed three-dimensional structures with broadband, low loss, high refractive indices. The core ideas proposed have been used to generate a two-dimensional material that has been demonstrated in the terahertz regime to give significant enhancements in refractive index [26]. To tailor the value of the refractive index Choi et al. [26] proposed controlling the degree of polarization and magnetization by using a strongly coupled, thin 'I'-shaped metallic patch to maximize the effective permittivity ε while suppressing the diamagnetic effect.

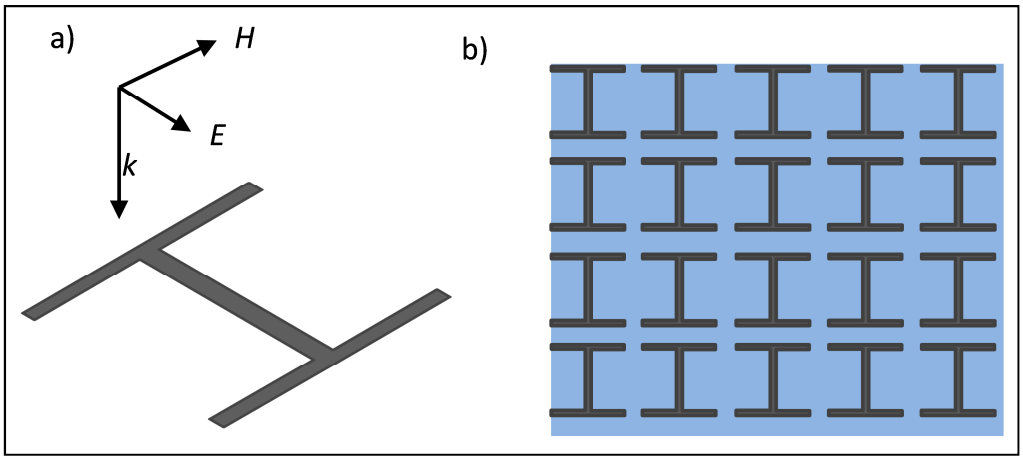

Figure 5: a) A thin 'I'-shaped metallic patch. The incident terahertz wave is directed downwards, with the polarization of the wave indicated by the arrows and b) a single layer of the metamaterial structure with the 'I'-shaped metallic patches arranged in a regular array and embedded in a dielectric material. Each 'I'-shaped patch is of the order 50 µm x 50 µm x 0.1 µm and each dielectric layer is approximately 2.5 µm thick.

Single and multi-layered structures were measured and significant index enhancement was seen in the terahertz regime, however, this two dimensional material is, by its nature, anisotropic. In this thesis we investigate one of Shin's proposed three dimensional geometries experimentally (an array of close packed cubic elements of cross-linked square metal plates), and confirm that it does indeed result in a broadband, low loss, isotropic high refractive index material.

Whilst the potential use of controllable positive refractive index materials in transformation optics based systems is clear [27] [28] [29], high index material may also be used in lithographic systems where increasing the refractive index

can improve the resolution of the processes [30]. A practical example of this can be found in the production of computer chips where using a high index lens can reduce the size and increase the quality compared with that which is currently available. In the microwave regime other applications of high refractive index materials include micromachined patch antennas, where a higher index substrate allows the miniaturisation of the patch antenna [31], and beam splitters and diverters [4] where a variable index is used to direct the electromagnetic energy. As well as the requirement for high refractive index materials in transformation optics based systems it is clear that there is also a requirement for anisotropic materials where the permittivity and permeability of the material is controlled in different directions through the material. Layered metamaterials which are anisotropic in two dimensions are routinely used but a three dimensional metamaterial in which the electric and magnetic properties can be controlled in three dimensions will provide significant flexibility which may beneficial for particular applications.

1.3 Chapter Summary

Chapter 1 has given a brief overview of electromagnetic metamaterials deliberately focussing on broadband, low-loss, three-dimensional structures. It is noted that the structural method proposed by Shin et al. [1] to control permittivity and permeability has been demonstrated experimentally for a two-dimensional structure in the terahertz regime [23]. In this thesis we further investigate the three-dimensional metamaterial structures and experimentally verify results previously shown theoretically by Shin et al.. Investigation and measurement of these structures requires EM modelling and measurement techniques specific to this class of structure, which are detailed in Chapter 2.

2 Modelling and Measurement Methods

This chapter details the electromagnetic modelling and measurement methods used to investigate the EM characteristics of the cubic array structures. The finite element method (FEM) modelling tool is firstly introduced and then used to investigate the EM response of an array of cubes (see Figure 6). The permittivity and permeability are extracted from the EM response and compared to assess the effect of changing the element structure and spacing. This chapter also details sample fabrication and the measurement method including stripline measurement and characterisation technique.

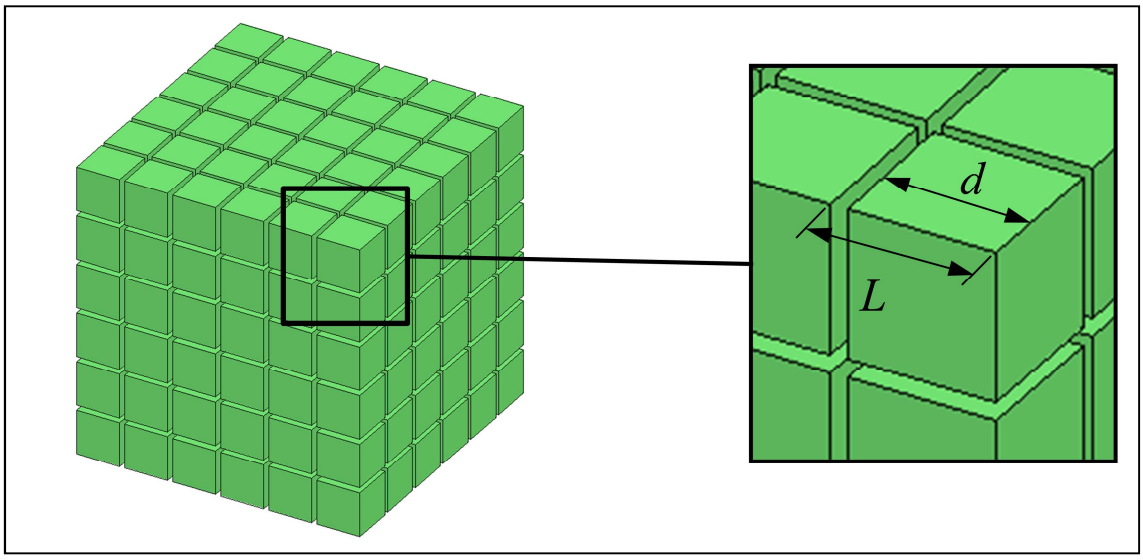

Figure 6: Illustration showing the construction of a simple array of cubes (inset exploded view of one unit labelled with the array spacing L and the cube dimension d).

2.1 EM Modelling using HFSS

The modelling in this thesis has been performed using a commercial finite element method (FEM) software package HFSS [32]. HFSS is a three-dimensional full-wave electromagnetic (EM) field simulator. This software package was chosen on account of the accuracy of its full field solver, combined with the flexibility of the adaptive tetrahedral meshing, which allows any arbitrary 3D geometry to be modelled, and in addition it has a well-developed CAD-based user interface.

HFSS uses the FEM modelling method, which in turn uses volume discretisation, dividing up the geometry being modelled into a 3D mesh of small tetrahedra. Maxwell's equations are transformed into a matrix form and solved for each mesh element. The accuracy of the field solution is dependent on the density of tetrahedral elements, with the greatest density of elements required where the gradient of the field is highest.

HFSS uses an iterative process to create the mesh of tetrahedra within the unit cell. HFSS creates an initial mesh based on the spatial resolution within the geometry and the refractive index of the media. The fields are then calculated within the mesh elements at the user defined solution frequency. An adaptive process is then performed where the number of mesh elements is increased with new elements being created where the field gradient is largest and more resolution is needed to accurately model the electromagnetic response. This process is then repeated until a specified convergence target is reached. The model may be seeded with mesh points by the user in areas where a finer mesh is likely to be required in order to minimise the number of iterations carried out by HFSS. A 2D representation of an example mesh through the unit cell used to model the structure is shown in Figure 7.

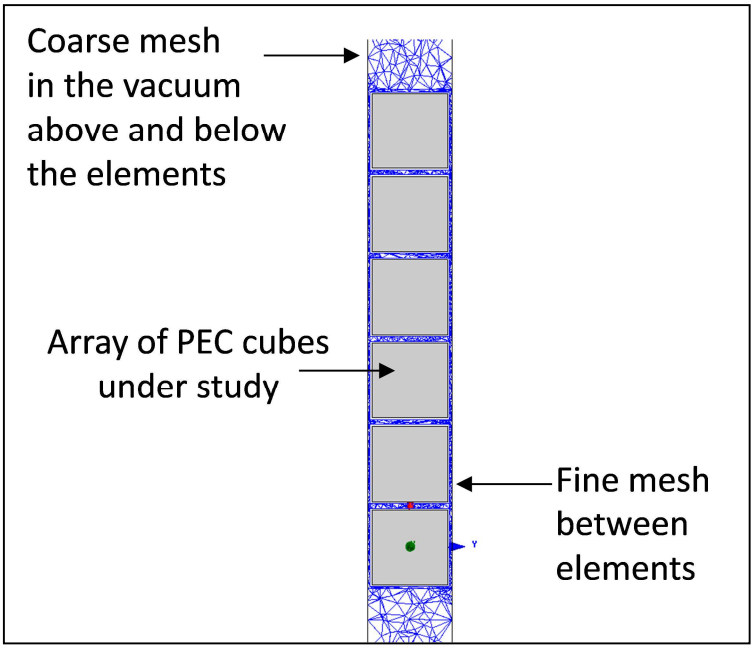

Figure 7: A two dimensional representation of a mesh through the array of cubes.

The modelling in this thesis concerns the responses of an array of cubic elements to an incident plane wave. The array is modelled as a periodic structure to simulate a 'slab' of material of infinite extent in the *xy*-plane and a finite number of layers in the *z*-direction.

For periodic structures a periodic master/slave boundary is used in HFSS. These boundaries ensure that fields on the master/slave are identical to that on the slave/master boundary. Using master/slave boundary conditions reduces the model geometry to a single unit cell, thereby reducing the volume of the model and therefore reducing computational time accordingly.

The plane wave incidence on the array is modelled in HFSS using a driven modal solution with the waves being generated using Floquet ports. A Floquet port defines the fields in terms of diffracted orders and produces plane waves comprising a series of Floquet modes. Floquet ports can only be used with periodic structures and are defined on the incident and exit faces of the unit cell. An illustration of a unit cell including the master/slave boundaries and the Floquet ports is shown in Figure 8.

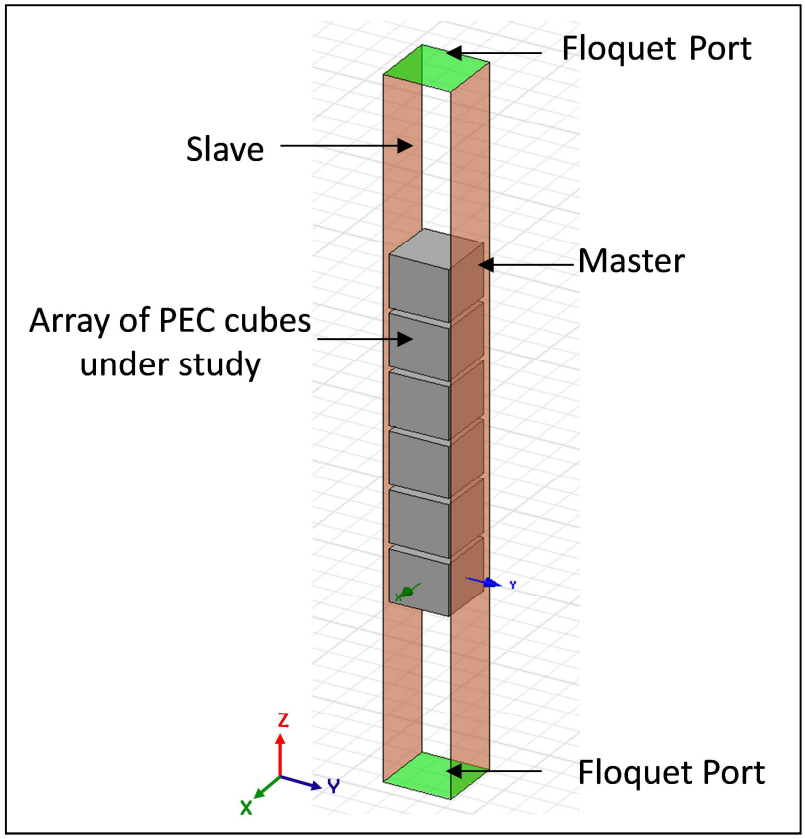

Figure 8: Illustration of geometry modelled in HFSS and the location of the Floquet ports and boundaries. It should be noted that the unlabelled boundaries (front and back) are also a pair of master/slave boundaries.

2.2 Typical HFSS Results for an Array of Cubes

An array of cubes was modelled to demonstrate how HFSS can be used to investigate the key characteristics of a 3D structure. The array consists of perfectly electrically conducting cubes suspended in a vacuum characterised by the lattice periodicity, *L*, and the cube dimension, *d*, as shown in Figure 6.

The HFSS software models transmission and reflection of a plane wave incident with the *k*-vector in the *z* direction through an array of cubes of infinite extent in the *xy* plane but only six elements deep in the *z* direction. A six layered structure with a period of 5 mm and a cube dimension of 4.5 mm was modelled from 0.6 GHz to 20 GHz, and the transmission and reflection response is shown in Figure 9.

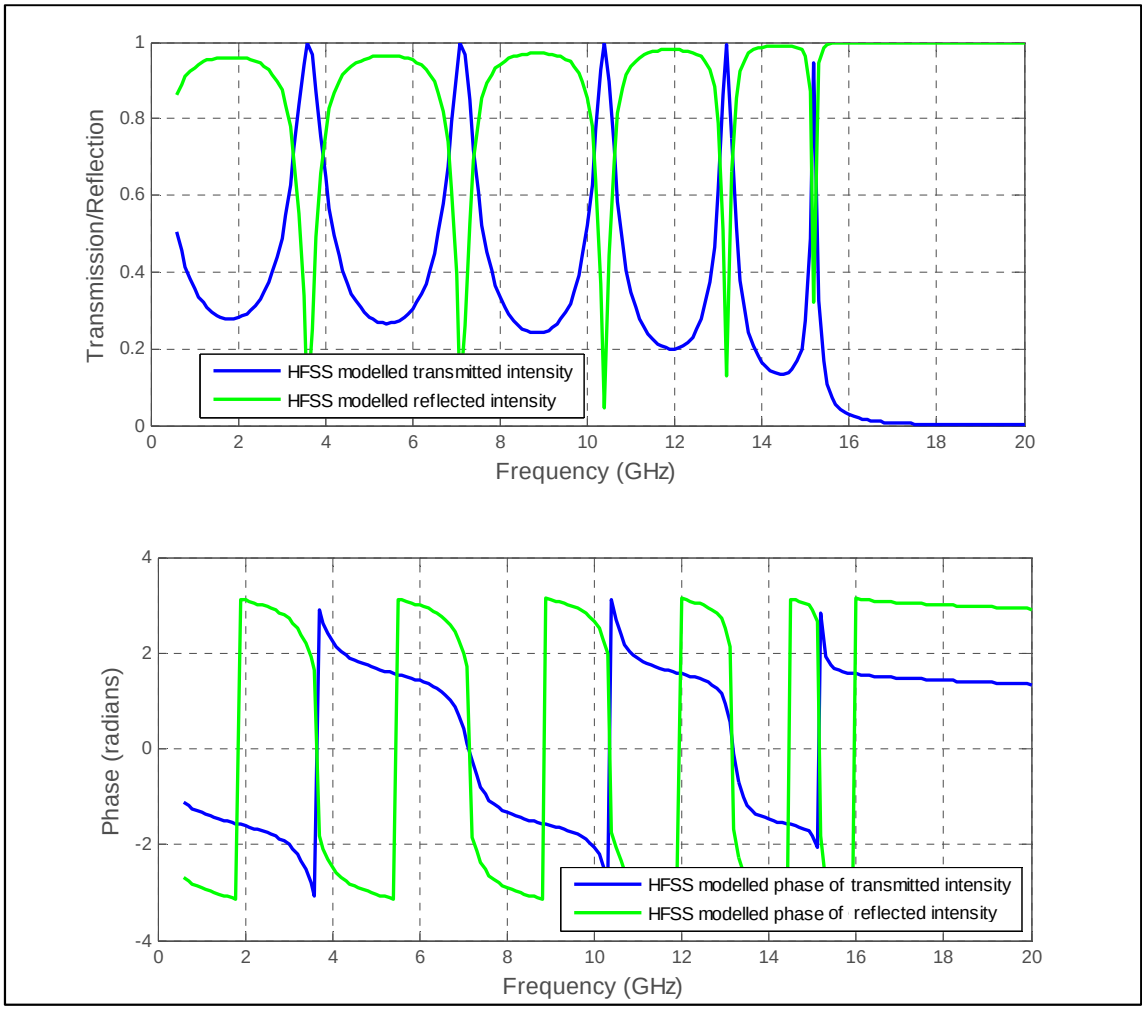

Figure 9: Plot showing the magnitude and phase of transmission and reflection through a six layered array of cubes between 0.6 GHz and 20 GHz.

The transmission and reflection responses show a clear modal characteristic with six modes, corresponding to the number of discrete layers of the structure in the direction of propagation (in this case the *z* direction). The Fabry-Perot-like (standing wave) resonances are due to interference between reflections from the front and back faces which result in transmission maxima and reflection minima. For a non-dispersive material these resonant features would be equally spaced in frequency. It is clearly seen in Figure 9 however, that the array structure becomes more dispersive as the band-gap is approached. The band gap will occur when the period of the array is equal to a quarter of the effective electromagnetic wavelength within the structure. This indicates that the period of the array, at the frequency at which the band-gap occurs, is no

longer much smaller than the wavelength in the material and can therefore no longer be considered to be in the metamaterial regime.

As well as being able to obtain the predicted transmission and reflection response of the system, HFSS was also used to visualise the electromagnetic fields and currents within the structure. This proved very useful in investigating the mechanisms involved and explaining certain characteristics of measured and modelled responses. Figure 10 shows typical HFSS plots of the electric field and magnetic field, here at 7.1 GHz associated with the array of cubes modelled above.

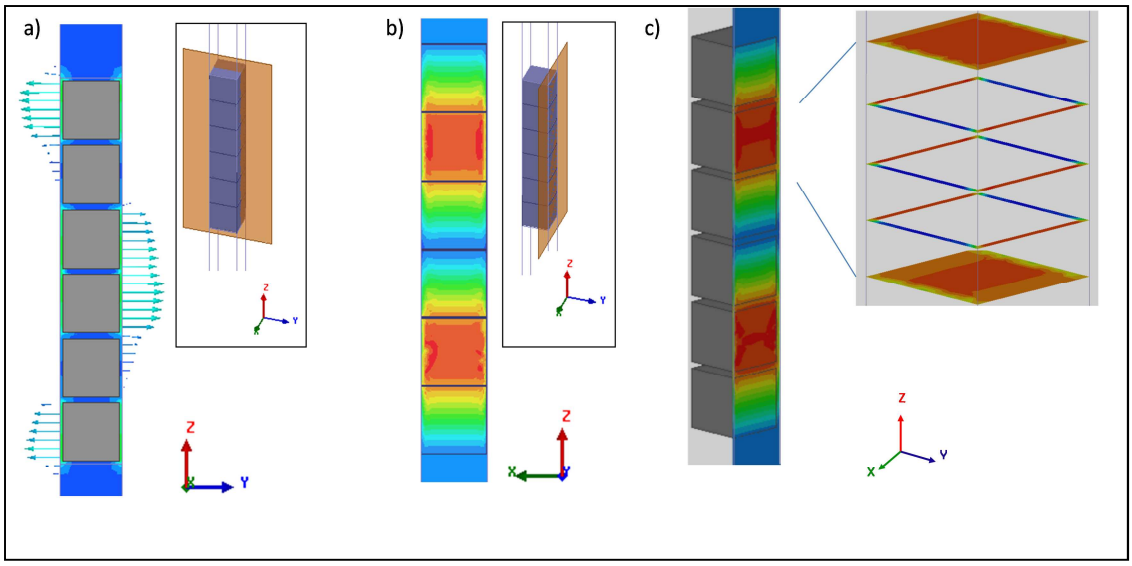

Figure 10: Typical field plots generated using HFSS of a) electric field, b) & c) magnetic field for a six layered array of solid PEC cubes with a period of 5 mm and a cube dimension of 4.5 mm subject to an incident plane wave in the *z*-direction with the E field in the *y*-direction. The fields plotted are the time averaged E and H field with the red representing a high magnitude through to blue representing a low magnitude. The arrows indicate the direction of the E field.

2.3 Extracting the Effective Permittivity and Permeability of the Structure

A key part of this thesis is concerned with how shaping individual elements within a structure affects the effective EM properties of the material. It is therefore important to be able to extract the effective permittivity and permeability from the reflection and transmission responses. The HFSS software calculates a full scattering matrix consisting of complex scattering parameters (S-parameters) which provides a complete description of the two

port system relating both the power transmitted to and reflected from the two ports. From the S-parameters the effective permittivity and permeability can be extracted using the Nicholson-Ross-Weir algorithm [33, 34].

Using a simple algebraic manipulation or the three layer Fresnel equation the Nicholson-Ross-Weir (NRW) algorithm uses measured or simulated complex transmission and reflection coefficient, frequency and thickness of the sample to determine the effective complex permittivity and permeability.

Suppose that a plane wave is incident on a structured slab as shown Figure 11, then provided the period of the structure is much smaller than the wavelength in the structure, then the structure can be considered equivalent to a homogeneous material with an effective permittivity and permeability.

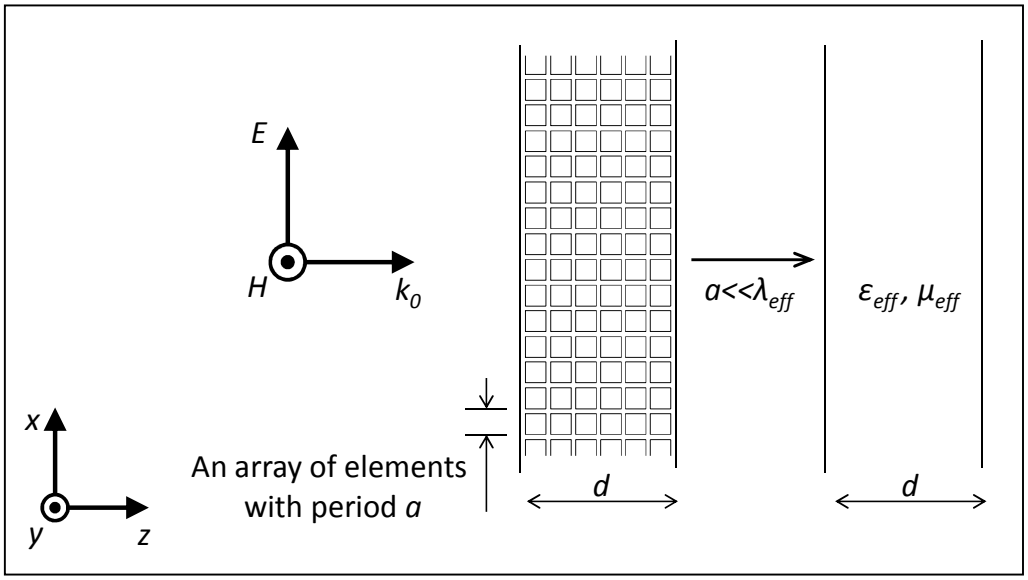

Figure 11: Characterization of the structured array of elements as a homogeneous material with ε_{eff} and μ_{eff} when a plane wave is normally incident on the structure. The structure is infinite in the *xy*-plane but a finite thickness in the *z*-direction (in this case six elements).

The scattering parameters can be formulated as follows:

$$S_{11} = \frac{(1 - z^2)R}{1 - R^2 z^2} \tag{2}$$

$$S_{21} = \frac{(1 - z^2)R}{1 - R^2 z^2} \tag{3}$$

$$R = \frac{\eta - 1}{\eta + 1} \tag{4}$$

$$z = e^{-ink_0 d} \tag{5}$$

Where $n = \sqrt{\varepsilon_{eff}\mu_{eff}}$ and $\eta = \sqrt{\frac{\mu_{eff}}{\varepsilon_{eff}}}$, define the refractive index and impedance respectively, R is the reflection coefficient across the first boundary between free space and the structure, k_0 is the free-space wave number, and d is the thickness of the structure in the z-direction.

Within the derivation of the NRW algorithm equations (2) and (3) are inverted to give:

$$\boldsymbol{\eta} = \pm\frac{(1 + s_{11})^2 - {s_{21}}^2}{(1 - s_{11})^2 - {s_{21}}^2} \tag{6}$$

$$z = \frac{s_{21}}{1 - s_{11}\left(\frac{\eta - 1}{\eta + 1}\right)} \tag{7}$$

$$n = \frac{1}{k_0 d}\ln(z) \tag{8}$$

The intrinsic problem with the NRW technique relates to the electrical thickness of the sample. Since the phase of the wave is periodic with a period of 2π, this causes ambiguity in the extracted results as seen in equation (8) and further explained in [35]. This ambiguity is shown in Figure 12, with each plot of the extracted index corresponding to a different root of the phase factor equation used within the algorithm. It can be seen that the first root of the equation (m = 0) corresponds with the lowest frequency solution. We assume the extracted index is continuous and can therefore use the plot of extracted index to select the correct root (value of m) to use for each frequency. This removes the ambiguity from the NRW algorithm which is then used to plot the extracted permittivity and permeability (Figure 13). It should be noted that the extracted values are not valid in the band gap region, which in this case is above 15 GHz.

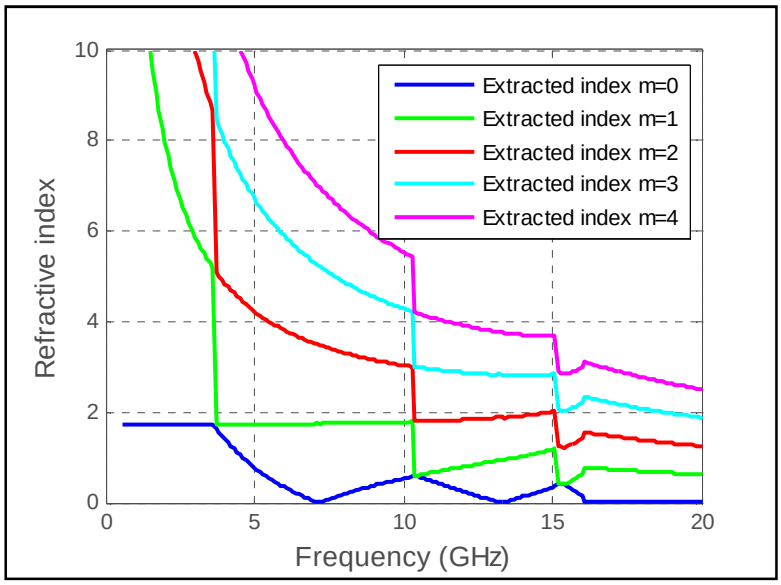

Figure 12: Plots showing the different branches of extracted refractive index using the Nicholson-Ross-Weir extraction method.

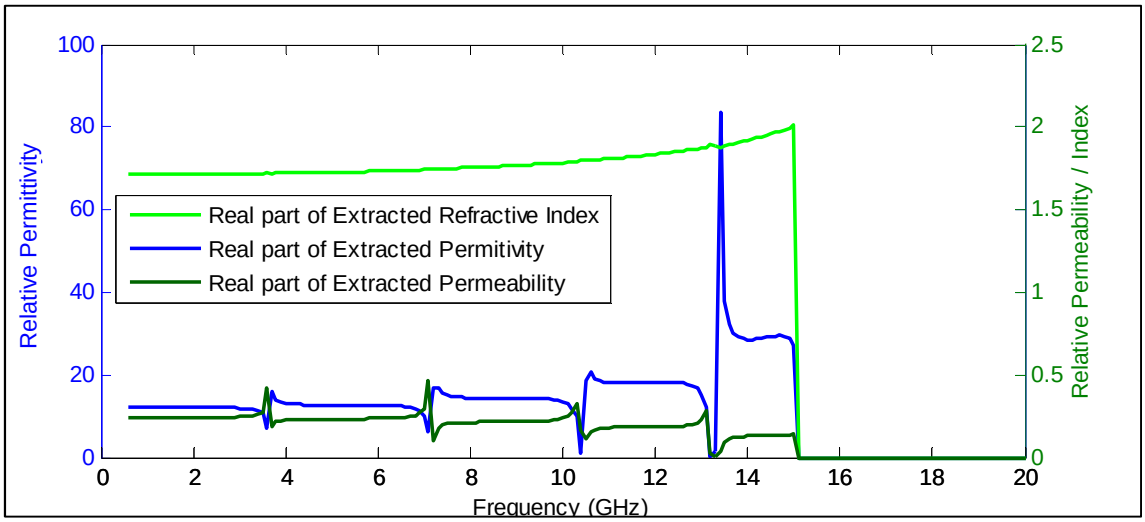

Figure 13: A plot showing the extracted refractive index, permittivity and permeability for an array of cubes with a period of 5 mm and a cube dimension, d, of 4.5 mm.

Figure 13 shows the real part of the effective permittivity, permeability and index illustrating a consistent value for the index over the range of interest (below 15 GHz) but clearly showing unacceptable variations in the effective permittivity and permeability. These strongly localised (in frequency) variations correspond to the modal frequencies of the structure where the reflected intensity is at a minimum, which effectively reduces the four equations used in the NRW algorithm to just two, which in turn causes the algorithm to break down. The

problem arises when the impedance of the sample under test is either close to unity or very large. The structures studied in this thesis suffer from this problem since the permittivity is expected to be very high, while the permeability is expected to be very low, leading to a large impedance mismatch and correspondingly small transmission coefficient.

With some of the structures investigated within this thesis having modes spaced much closer together it was found that such inconsistencies with the NRW algorithm could dominate so it was necessary to use an alternative method.

Using the low frequency value from the NRW algorithm, the transmission response for an equivalent dielectric ($\varepsilon = 10$, $\mu = 0.2$) is compared to the predicted response of the array of cubes in Figure 14. Good agreement is seen below 8 GHz, with the dispersive nature of the structure manifesting itself as the band-gap is approached. Matching both the real and imaginary parts of the transmission and reflection response forms the basis of the alternative method for effective parameter extraction. The assumption is made that the permittivity and permeability are non-dispersive over the frequency range of interest, which means that rather than fitting data at each individual frequency value, as the NRW method does, all of the frequency dependent data can be used. A fitting routine developed by Ian Hooper of the University of Exeter Electromagnetic and Acoustic Materials group was used to fit the real and imaginary parts of the reflection and transmission coefficients to a three-layer Fresnel model (equations 2 - 5). The sum of squares between the model and experimental data was used as the objective function with the only variables being the real and imaginary parts of the permittivity and permeability (this method is similar to that used by Abbas et al. [36]).

In this thesis the NRW is used for the extraction of parameters from modelled data (in the frequency range over which the structure can be considered non-dispersive) but because of the limitations described above the alternative methods of using a numerical fitting routine was used to extract the permittivity and permeability from the measured data.

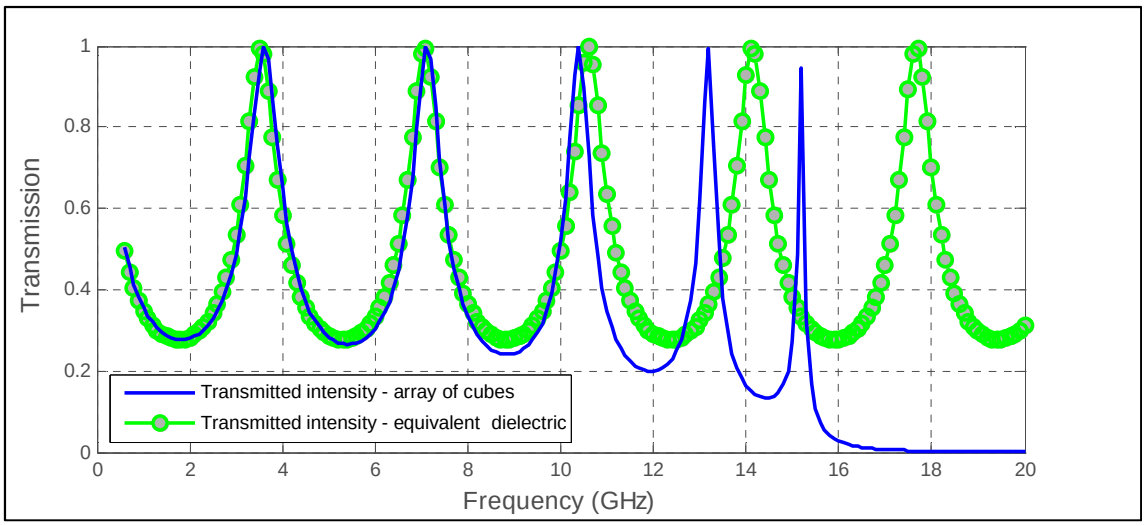

Figure 14: A comparison of the transmission response of an array of cubes and the equivalent non-dispersive dielectric.

2.4 Measurement and Characterisation of an Array of Structured Elements

This section details the fabrication and measurement of array structures constructed from cubic and shaped structured elements. (It should be noted that much work was carried out on different fabrication techniques by Alex Patterson and Ruth Lovelock, two summer students working within the University of Exeter Electromagnetic and Acoustic Materials Group).

2.4.1 Sample Fabrication

The HFSS modelling detailed in Chapter 2 is of PEC elements suspended in a vacuum. In practice the array is realised with metallic elements suspended in a low loss dielectric. The difficulty in manufacturing a sample to be measured is the large number of elements that need to be exactly positioned in a dielectric to form an array of elements.

The first option considered for the manufacture of the sample was additive layer manufacturing (ALM). ALM is the process by which components are manufactured one layer at a time. There are various different procedures such as stereo lithography, 3D printing and selective laser sintering that can be used to manufacture components in metals and plastics.

The initial idea was to use ALM techniques to build up the sample from layers of metal and dielectric, with each layer consisting of isolated metallic patches in a dielectric sheet. ALM is a rapidly maturing technology but techniques that combine metallic and dielectric materials in a single structure are not yet widely available.

Given the financial and time constraints of this work, ALM techniques were not used to create the entire sample, but were used to manufacture the individual structured elements. The measurement samples were fabricated by individually manufacturing the cubes and structured elements and arranging them into an array.

The individual elements, consisting of six plates connected by three orthogonal wires using an additive layer rapid prototyping technique, are made conductive by coating the elements with nano-crystalline copper. The metallic cubes were manufactured by machining the cubes from solid copper.

Two methods were used for aligning the elements into a periodic array. A compartmentalised tray produced using ALM techniques gives a uniform separation and keeps the elements isolated from each other.

Figure 15 shows the assembly of one single layer of the structure. Unfortunately limitations in the resolution of the ALM process result in there being a minimum element spacing that can be achieved.

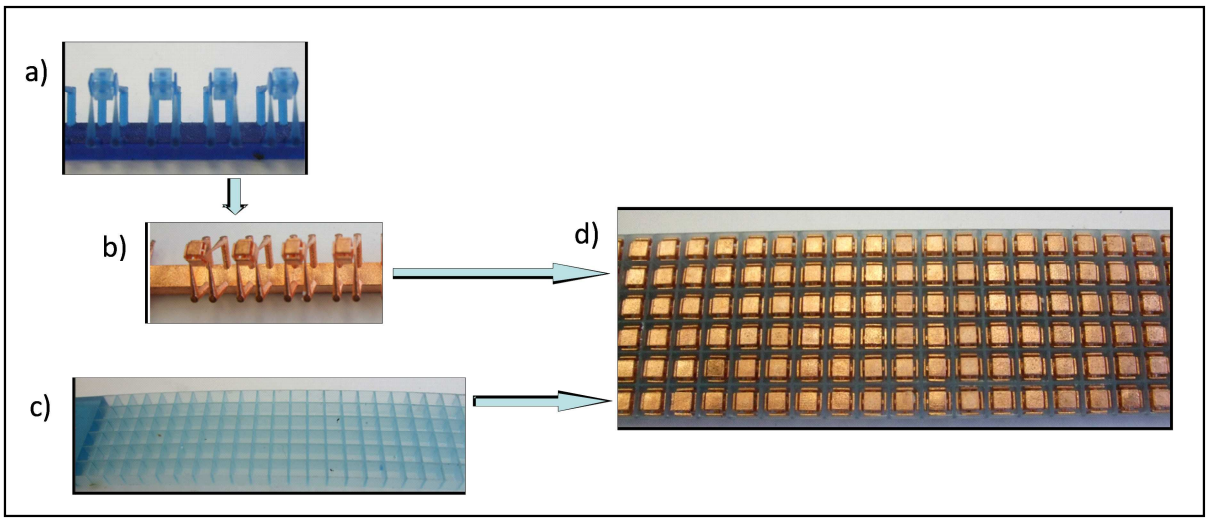

Figure 15: Photographs showing: (a) the elements fabricated using an additive layer rapid prototyping technique, (b) the elements coated in nano-crystalline copper, (c) the compartmentalised tray fabricated using an additive layer rapid prototyping technique, and (d) the assembled 6-strip structured metamaterial sample.

An alternative way of arranging elements used square acrylic patches adhered to the outer surfaces of the cubic and structured elements. Each layer of the structure was held together with a band of PTFE as shown in Figure 16. The advantage of this approach over the compartmentalised tray was that the elements could be arranged closer together, but the disadvantages were that the sample was more fragile and the assembly of large layers more difficult.

(It should be noted that help was received with the intricate and time consuming job of assembling the arrays of structured elements and cubes by Ian Hooper from the University of Exeter Electromagnetic Materials Group).

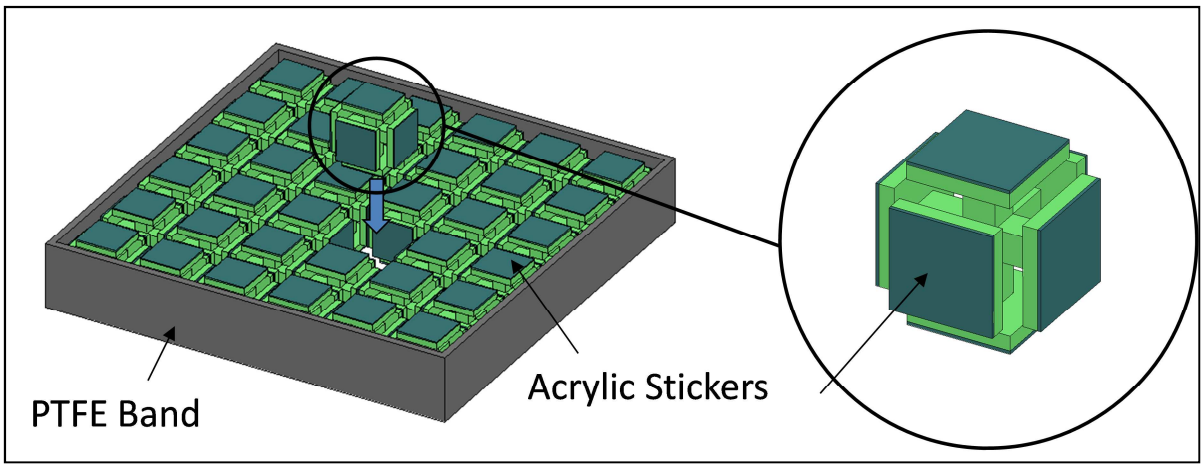

Figure 16: Schematic showing a layer of copper structured elements separated by acrylic patches and held together with a PTFE band.

2.4.2 Measurement Techniques

To carry out EM characterisation of the structure, transmission and reflection measurements are required. The first methods considered for transmission measurements were free space measurements where transmit and receive antennas are positioned at either side of the large 'slab' of material and the transmission and reflection measured directly. Unfortunately a very large sample is required to avoid edge effects.

To simplify sample manufacture and to reduce the size of sample it was decided to use PEC boundary conditions. FEM modelling in Chapter 2 (see Figure 10a) showed that with external radiation applied with the *k*-vector in the *z*-direction and the electric field in the *x*-direction then the electric field between neighbouring elements is largely normal to the faces of the cubes. This means that rather than fabricating a 3D structure, all that is required is to place a 2D layer of cubic units between parallel PEC plates. Thus the third dimension is replaced by the PEC boundaries acting as 'mirrors' so that a 2D sheet of metamaterial placed between PEC plates acts, to a first approximation, as a 3D structure as illustrated in Figure 17. In effect, the PEC boundaries proposed for the measurement act similarly to the master/slave boundaries in the HFSS modelling.

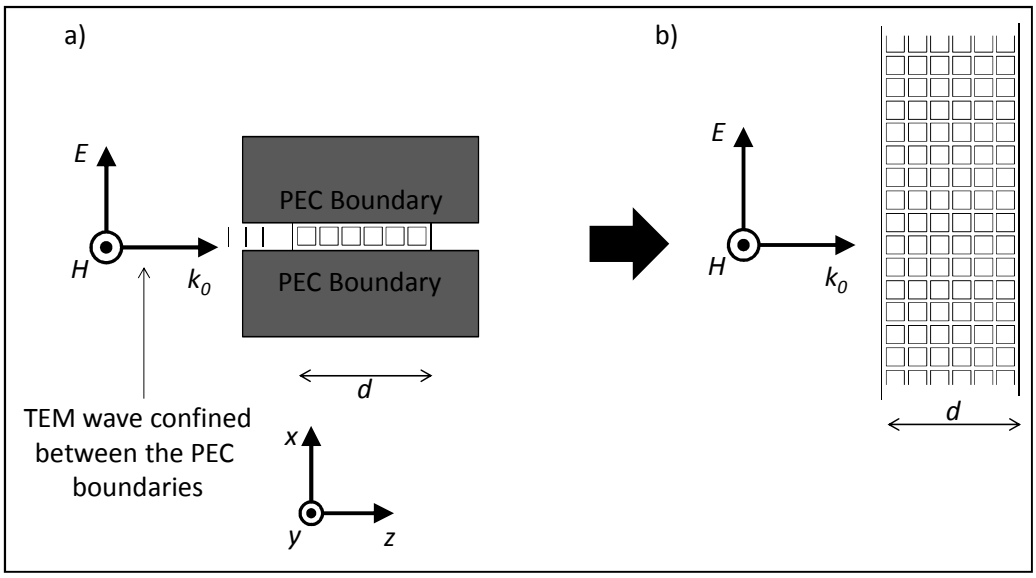

Figure 17: A diagram illustrating the use of PEC boundary conditions to simulate the response from a larger slab of material. An array of elements (1xnx6), shown in (a) gives an equivalent response to an incident plane wave to that from a much larger (infinite) array (∞xnx6). Where n is a finite number a represents the width of the sample.

Figure 18 shows the modelled transmission response of an array of cubes with both master/slave and PEC boundary conditions. It should be noted that the PEC boundary conditions are only on the boundaries that are normal to the incident E-field.

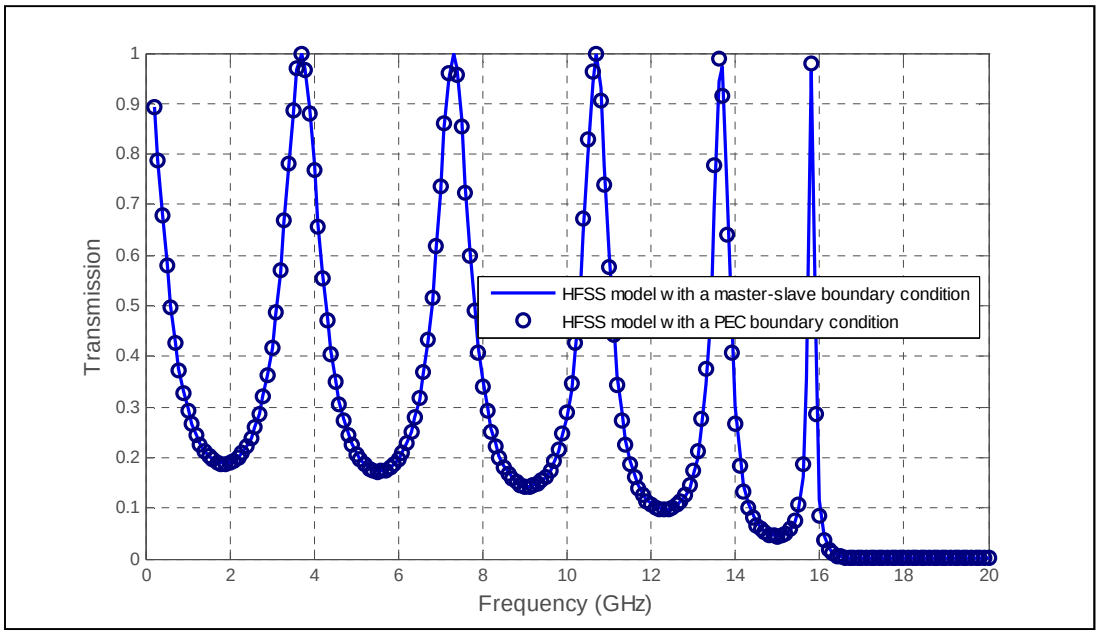

Figure 18: Plot showing the modelled transmission response through a six layered array of cubes with master-slave periodic boundary condition compared with the response from the same model with the master-slave boundary replaced by a PEC boundary condition on the boundaries normal to the electric field of the incident plane wave.

Given the limitations on the size of the fabricated sample the stripline transmission line technique was considered an ideal candidate for the characterisation of the 3D metamaterial structure. The stripline geometry has PEC boundaries that are used to simulate the transmission through an infinite 'slab' of material as described above.

(It should be noted that during the development of stripline measurement technique much of the formative work was carried out by Ruth Lovelock and Ian Hooper from the University of Exeter Electromagnetic Materials Group).

The stripline comprises a centre conductor sandwiched by the sample being measured between a pair of ground planes. It can be thought of as a flattened coaxial cable with a guided wave being supported between the centre conductor and ground planes which is transverse electric and magnetic (TEM) in nature. The guided wave has a strong vertically polarised electric field component with the electric field being orthogonal to the centre conductor surface. Since there is no low frequency cut-off for such a wave it is supported over a broad frequency range. In practice the stripline device is connected via a coaxial cable and coaxial connector to a calibrated vector network analyser and when a sample of unknown permittivity and permeability is placed symmetrically between the centre conductor and the ground plane the complex reflection and transmission coefficients can be measured. For accurate measurement of the amplitude and phase of reflection and transmission it is necessary to minimise the impedance mismatches throughout the system. A typical stripline is shown in Figure 19. The characteristic impedance of this arrangement is governed by geometry and the relative permittivity of the sample. An empirical formula [37] for the impedance Z_0 of the transmission line is:

$$Z_0 = \frac{30\pi}{\sqrt{\varepsilon_r}} \ln\left[\frac{b}{W_e + 0.441b}\right] \qquad (9)$$

where W_e is the width of the centre conductor, b is the separation of the ground planes (both in mm) and ε_r is the relative permittivity of the sample. Using this expression the geometry is tailored to match the impedance of the coaxial cable

used, in this case 50 Ω. The stripline was designed to be impedance matched with the coaxial cables, connectors and Vector Network Analyser in its unfilled state with the sample being introduced in the central region of constant cross section.

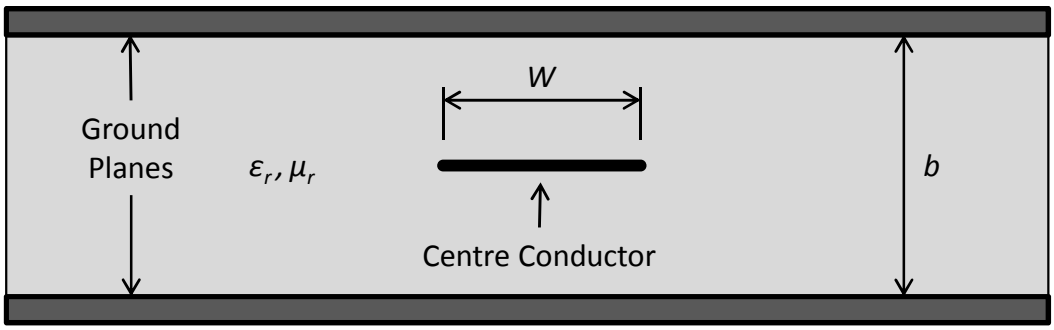

Figure 19: Diagram of a typical stripline showing the key geometrical parameters.

During the work detailed in this thesis two stripline devices were used. In the first device two layers of the structured metamaterial (See Figure 15d) are positioned between a central conductor and ground planes in the region of constant cross-section and are aligned so that the sample is orthogonal to the direction of propagation of the TEM waves through the device as shown in Figure 20. This stripline arrangement is optimised using two transition regions, tapering both the centre conductor and the ground plane separation from the coaxial connectors to the main body of the structure. This ensures a smooth profile in impedance and minimises the mismatches within the structure. A Vector Network Analyser with time domain processing is used to further reduce the impact of any mismatches.

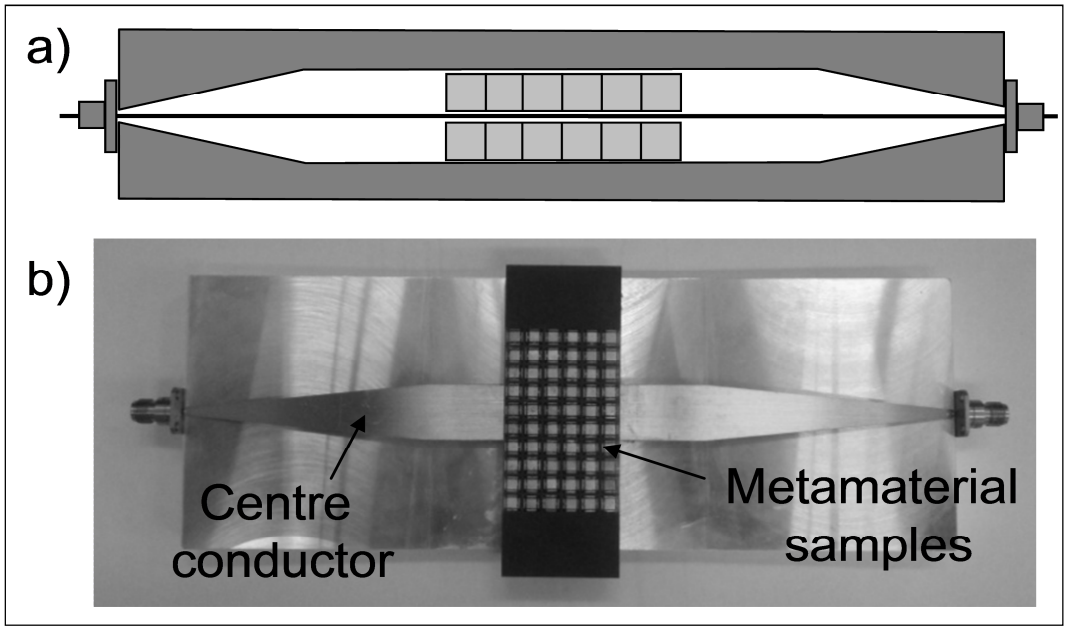

Figure 20: The stripline device. a) A side view schematic of the assembled device and b) a top view photograph of the device without the upper ground plane showing the alignment of the structured elements.

The device was designed to be impedance matched over as wide a frequency range as possible, with measurements eventually being taken from 500 MHz to 20 GHz. This resulted in a relatively long device, with a thin ground-plane and fine delicate coaxial connectors. The disadvantage of this stripline design was that the lack of robustness made it difficult to take accurate reference measurements without a sample present. This reference measurement along with phase measurements is required for the extraction of the effective permittivity and permeability.

The second device used, illustrated in Figure 21, was an existing device called a permeameter constructed by Ian Hooper and based on pioneering work by Barry in 1986 [38] which was constructed for the characterisation of loaded dielectrics over a lower frequency range. The device is much shorter, has more robust connectors and the geometric transition to the coaxial connector is achieved by only varying the width of the central conductor and not by changing the spacing between the ground planes.

The metamaterial 'sandwich' was characterised at low microwave frequencies (30 MHz to 4 GHz) in the same way as described above using this alternative stripline geometry.

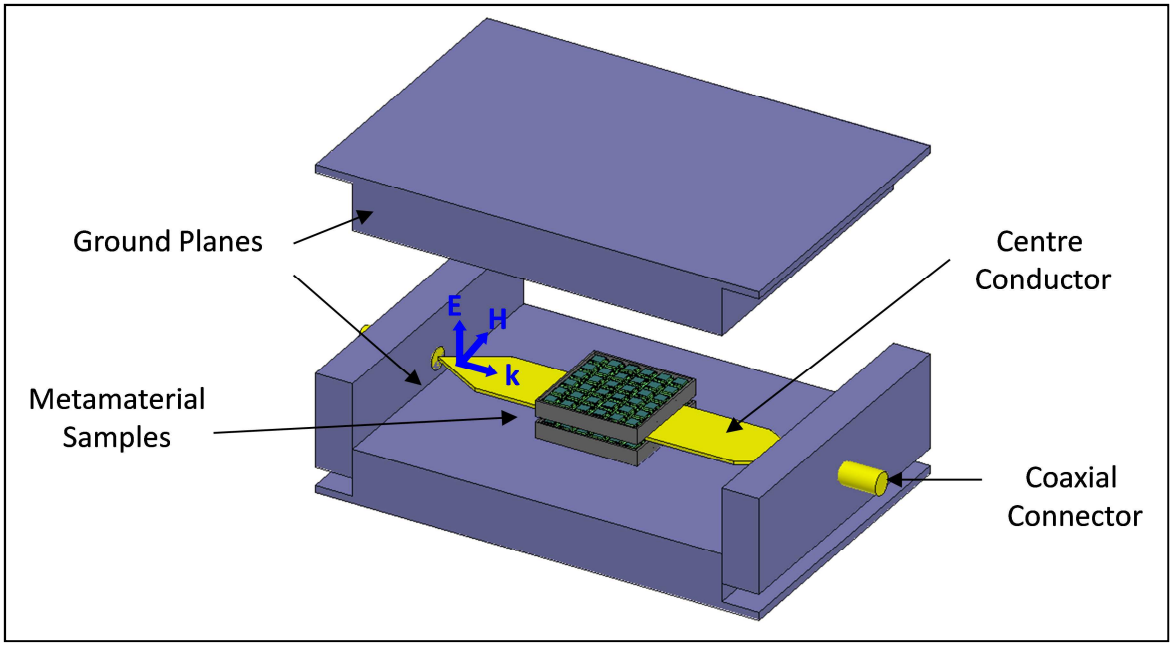

Figure 21: A schematic view of the modified stripline device.

2.5 Chapter Summary

The techniques detailed in this chapter were used to fabricate and measure arrays of structured elements and cubes. The transmission and reflection measurements are used to extract the effective permittivity and permeability so that the effect of element structure on the effective properties of an array of elements can be investigated. The results and analysis of the measurements taken are detailed in Chapter 3.

3 Measurement Results

The results of electromagnetic characterisation measurements of arrays of cubic and structured elements are presented in this chapter. Results are compared with FEM modelling of the measured samples and extensive discussion is provided to explain the characteristics observed.

The main aim of measuring the metamaterial structures was to confirm experimentally that shaping the individual elements of an array of elements can increase the effective index of the structure by reducing the area of the current loops while maintaining the capacitive effect between elements.

A stripline method for measuring permittivity and permeability to experimentally characterise the electromagnetic response of an array of cubes or structured elements was used, as detailed in Chapter 2.

3.1 Preliminary Results

Preliminary measurements were made of 180 structured elements 4.2 mm in dimension arranged in two (6×15×1) dielectric trays (see Figure 15) using the varying impedance stripline device shown in Figure 20. This method proved inconsistent and only a limited amount of usable data was gathered.

Figure 22 shows the normalised transmitted intensity for frequencies between 0.2 and 20 GHz measured through a six layered structure of shaped elements arranged in a dielectric tray using this test arrangement. The Fabry-Perot-like (standing wave) resonances seen are due to interference between the front and back faces which result in transmission maxima and reflection minima. The six layered structure has a group of six lower order modes terminating at about 7 GHz. There is then a distinct photonic band-gap between 7 and 17 GHz followed by weaker higher order modes which are less well defined.

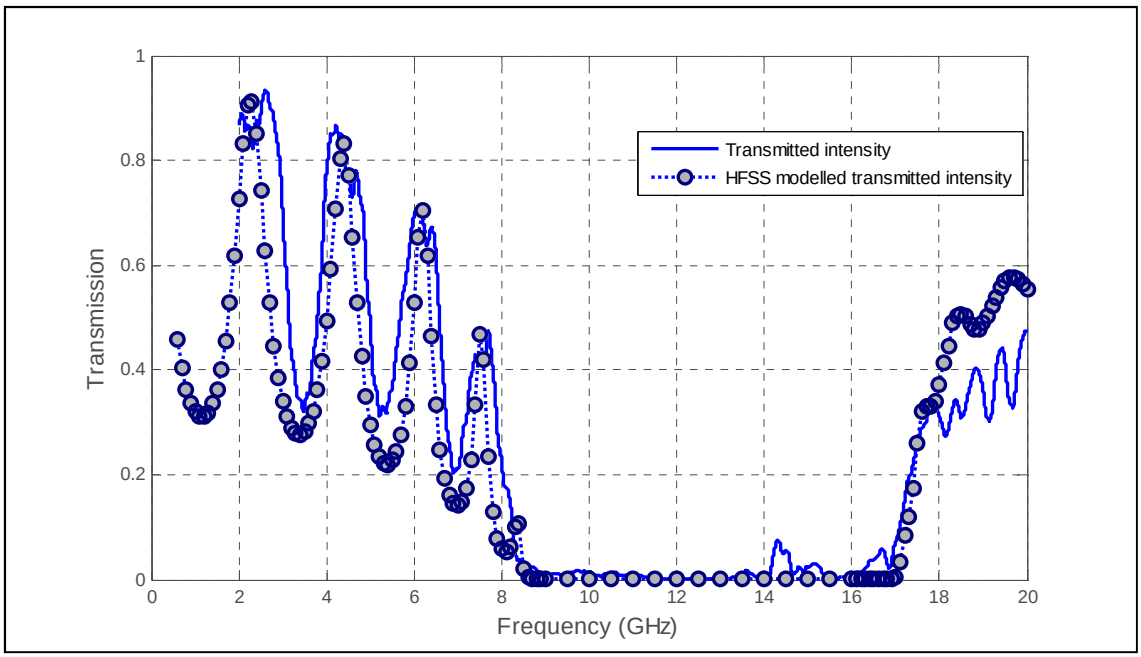

Figure 22: Measured transmission response through a six layered array of structured elements in the stripline geometry (full line), compared with HFSS model predictions (dashed line and symbols).

The EM response was modelled in HFSS with a plane wave incident having its *k*-vector in the *z* direction through an array of copper elements 4.2 mm in dimension (with an individual plate size of 2.8 mm × 2.8 mm) separated by dielectric spacers (300 μm thick, ε = 2.76 + 0.001i). The structure was modelled as being of infinite extent in the *xy*-plane but only six elements deep in the *z*-direction. A model fit was achieved by modifying the value of the dielectric constant of the dielectric spacer in the model to account for the inevitable air gap between elements present in the measured sample. The dashed line in Figure 22 is the best model fit to the data. Overall the features are all present, of the right level and occur at approximately the right frequency, although there appears to be a splitting of the modes which is likely due to interference asymmetries in sample manufacture. Note that the lowest frequency of the second band, which dictates the width of the stop band, is strongly dependent on the size and electrical properties of the dielectric filled gap between the elements.

The benefit of using this stripline device is that the impedance is well matched allowing measurement of transmission response over a wide frequency range.

The disadvantage however of this stripline device was that the lack of robustness made it difficult to take accurate measurements without a sample present. As noted above this reference measurement along with phase measurements is required for the extraction of the effective permittivity and permeability.

A different measurement technique was required to accurately extract the bulk properties from the measured response and to achieve a good comparison between the cubic and shaped elements.

3.2 Measurements Using the Modified Stripline Device

Using the permeameter constructed by Ian Hooper and based on pioneering work by Barry in 1986 [38] measurements were taken of an array of both cubic and structured elements.

(It should be noted that help was received in taking measurements of the element samples by Ian Hooper from the University of Exeter Electromagnetic and Acoustic Materials Group).

3.2.1 Measurement of an Array of Metallic Cubes

Sixty solid copper cubes 4.2 mm in dimension, arranged in two (6×5×1) layers, held together with a band of rubber of low dielectric constant, and separated by small acrylic stickers was measured using the permeameter device (see Figure 20). Figure 23 shows the reflection and transmission response from 100 MHz to 8 GHz. It should be noted that although the permeameter is only accurate up to 4 to 5 GHz because of the impedance mismatch at the higher frequencies, the device can be used to show general trends in the reflection and transmission response up to approximately 8 GHz. Similar to the preliminary measurement results the modal response of the layered array can clearly be seen. Within the frequency range measured, only the first four modes of the expected six lower order modes are to be found (see Figure 23).

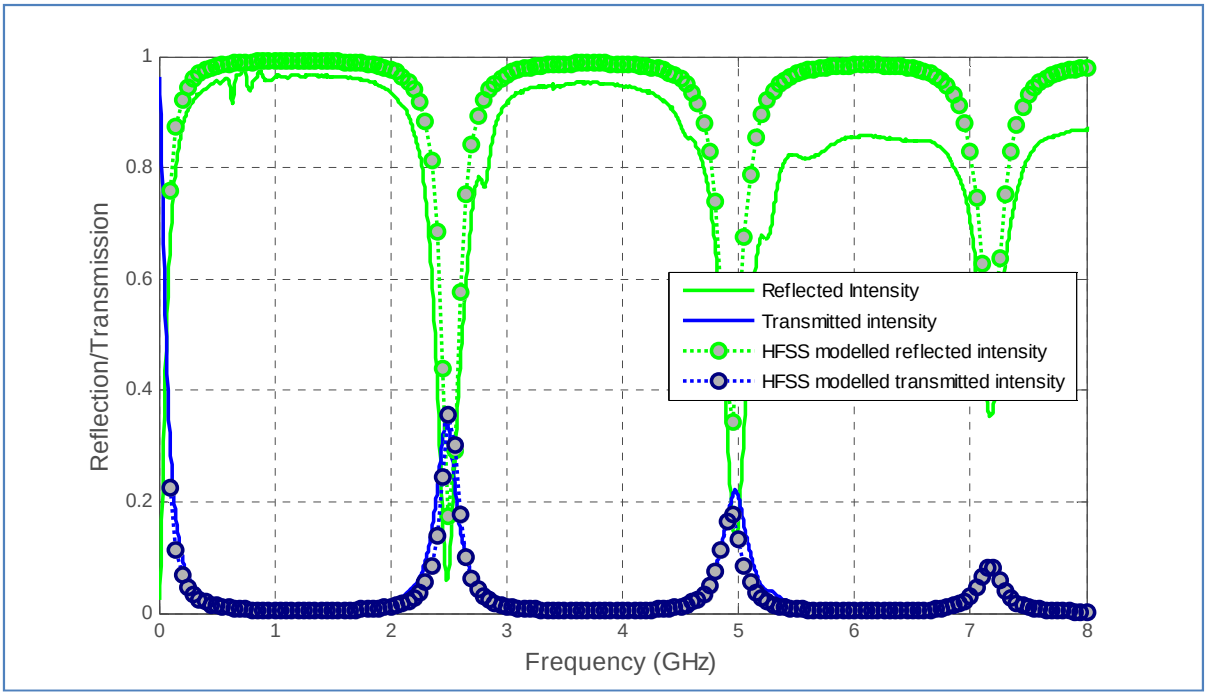

Figure 23: Measured (continuous lines) and modelled (dashed lines) reflection and transmission response for a six layered array of metallic cubes.

The EM response of the sample was modelled in HFSS with a plane wave incident having its *k*-vector in the *z*-direction through an array of solid copper cubes 4.2 mm in dimension separated by 85 μm thick acrylic (ε = 2.55 + 0.001i). The structure was modelled as being of infinite extent in the *xy*-plane but only six elements deep in the *z*-direction and was modelled from 0.6 GHz to 8 GHz. Model fits are the dotted lines in Figure 23 which generally show good agreement with all the modes present at the right frequencies and intensity, although the modes seem to be slightly wider in the measured data, probably due to the manufacturing tolerance in the structured sample..

The intensity of transmission and reflection at the modal frequencies for both the modelled and experimental results reduces at the higher frequency modes due to the loss in the system. The discrepancy in measured and modelled reflected intensity off resonance, particularly at higher frequencies is less easily explained but is likely due to the stripline no longer being impedance matched at these higher frequencies.

Figure 24 shows the frequency of each mode plotted for both the measured and modelled response with the modelled response being extended to include all six of the modes in the lowest band. It can be seen that the first four modes are roughly evenly spaced with the higher frequency modes becoming more tightly spaced showing dispersion within the structure. Although the structure is fabricated from non-dispersive materials the layered structure gives rise to a dispersive response. When the wavelength within the structure approaches the period of the array the response shows dispersion and when the spacing of the elements is equal to a quarter of the wavelength a band gap will be evident. As the frequency increases the onset of dispersion indicates that the structure is no longer in the metamaterial regime with wavelength no longer being much smaller than the period of the structure. In this case the structure can be considered non-dispersive up to approximately 4 GHz.

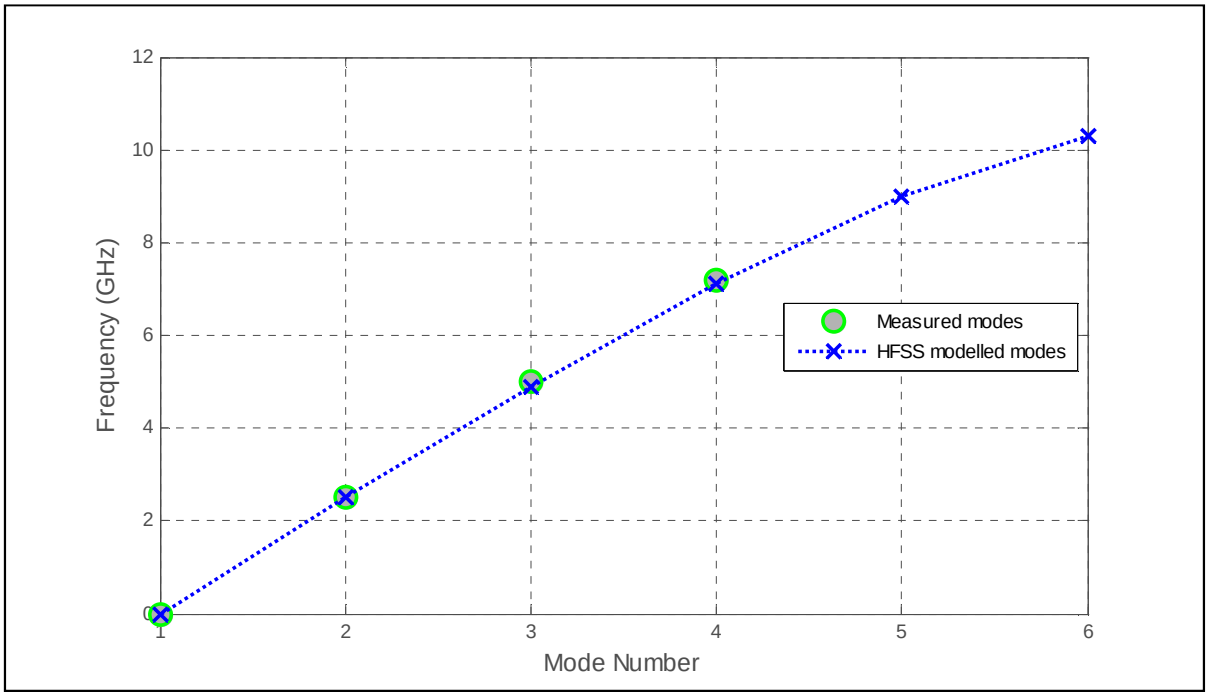

Figure 24: Plot showing the frequency of each mode for the measured and modelled responses of a six layered array of metallic cubes.

Over the frequency range for which the structure is considered non-dispersive the response of the structure is similar to that of an equivalent dielectric. A slab of non-dispersive homogeneous dielectric material would exhibit a response with modes equally spaced over the entire frequency range. In the frequency

range where the period of the structure << λ / *n*, it is valid to specify an effective permittivity and permeability which would also characterise the slab of equivalent dielectric. Permittivity and permeability values were extracted using a fitting routine developed by Ian Hooper of the University of Exeter Electromagnetic Acoustic Materials group which was used to fit the real and imaginary parts of the reflection and transmission coefficients to a three layer Fresnel model of the equivalent dielectric. Figure 25 shows the measured reflection and transmission compared with that of an equivalent dielectric with a permittivity of 49.5 + 1.53i and a permeability of 0.1, resulting in an effective refractive index of 2.25 + 0.04i. This result agrees reasonably well with the estimate (equation 1) of an ideal array of PEC cubes in a vacuum from the work of Wood and Pendry detailed in Chapter 1 [24] which yields a permittivity of 41, a permeability of 0.07 and an index of 1.77. (It should be noted that the lattice constant *l* is adjusted to take account of dielectric constant of the spacer in the calculation of the estimated permittivity ε_{eff} in equation (1)).

Note that the effective properties are assumed constant over the frequency range for which the structure can be considered non-dispersive (<4 GHz).

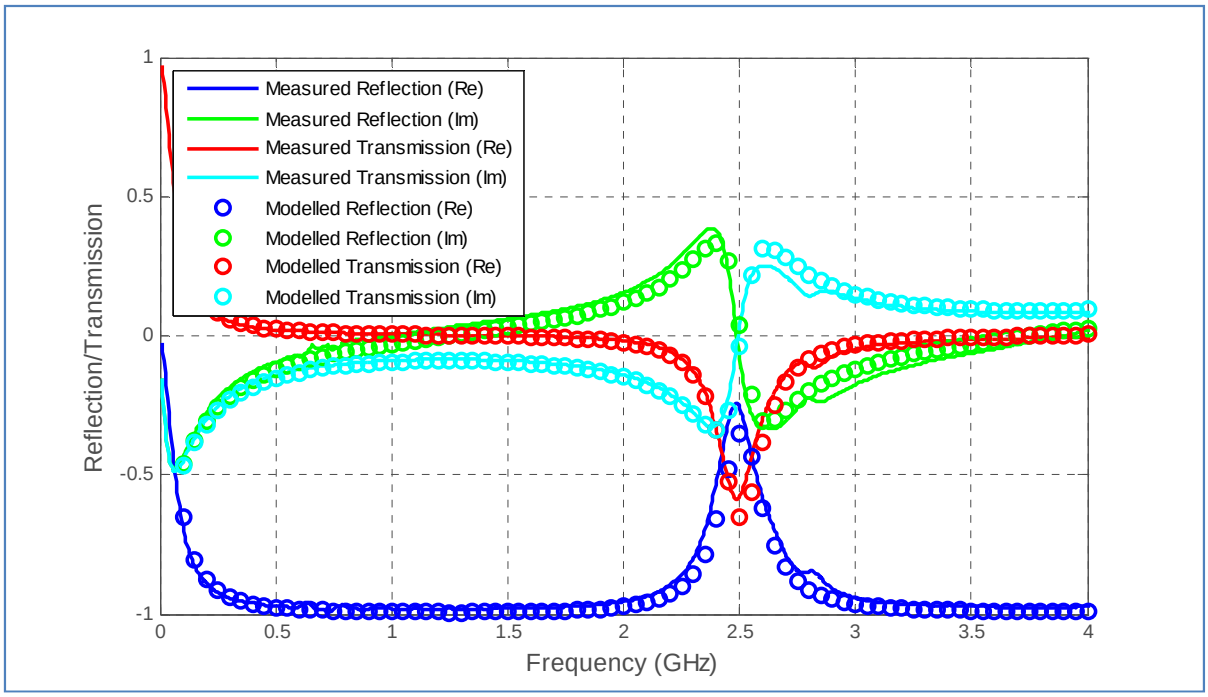

Figure 25: Comparison of the measured reflection and transmission with the modelled response of an equivalent material with ε = 49.5 + 1.53i, μ = 0.1.

To further investigate the characteristics of an array of cubes, FEM modelling was carried out of the EM response an ideal structure comprising of PEC cubes suspended in a vacuum. An ideal structure was modelled as key characteristics (particularly at higher frequencies) are more easily observed in loss-less structures.

The FEM software models transmission and reflection of a plane wave incident with the *k*-vector in the *z*-direction and the *E* field in the *y*-direction through an array of cubes of infinite extent in the *xy*-plane but only six cubes deep in the *z*-direction.

Figure 26 illustrates the electric field plots in the *yz*-plane through the centre of the cubes for each mode showing the electric field concentrated between the cubes primarily in the *y*-direction normal to the face of the cubes. The direction of the electric field is shown and the form of modes are clearly evident with the propagation of the electric field and therefore the effective permittivity being clearly governed by the capacitive effect between neighbouring cubes.

The magnetic field plots are illustrated in Figure 27 and Figure 28 which show the magnetic field concentrated between the cubes in the *x*-direction but unlike the electric field, the magnetic field can also be concentrated between layers of cubes in the *z*-direction (see Figure 28). The magnitude of the magnetic field is affected by the diamagnetic effect associated with the isolated cubes. The magnetic field produced by the induced currents on the cube opposes the incident magnetic field and therefore reduces the effective permeability of the structure.

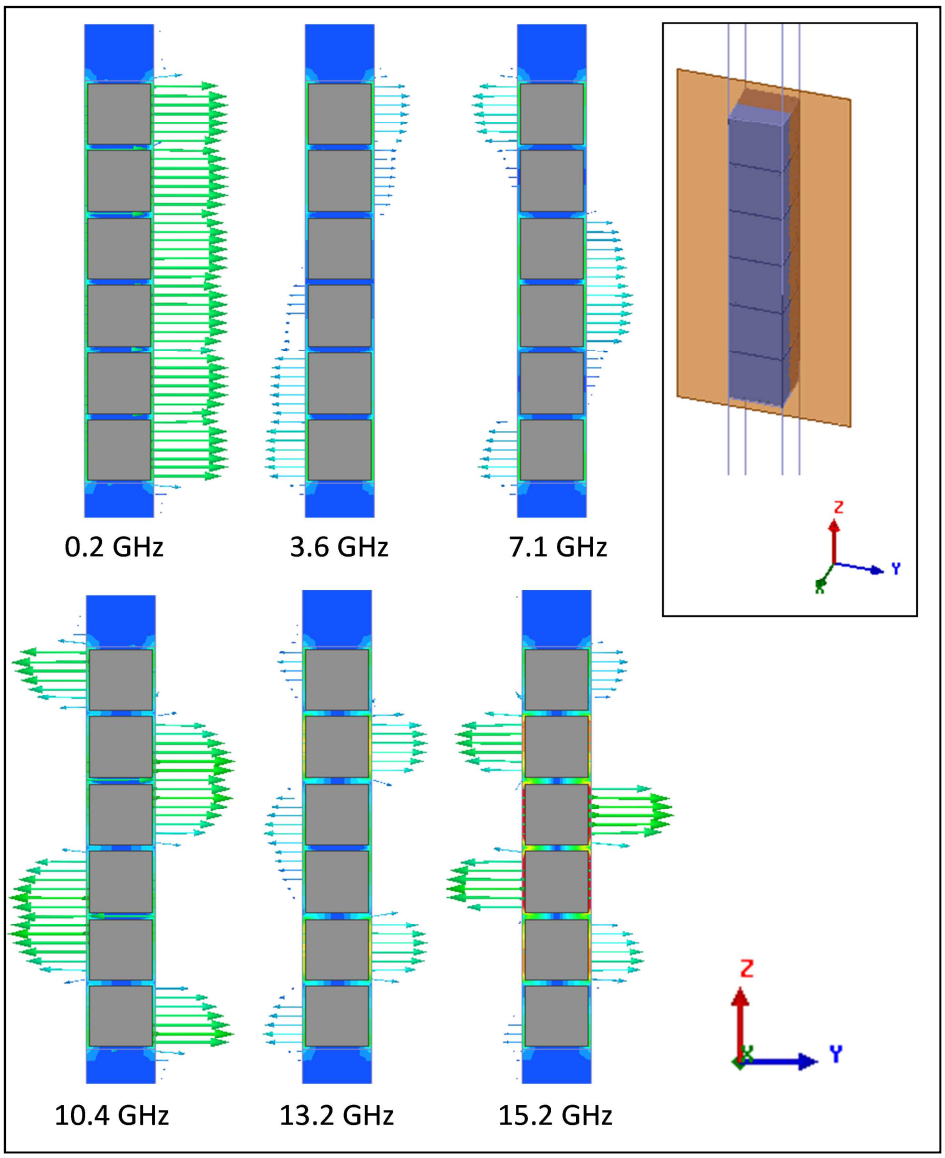

Figure 26: Electric field plots for an array of PEC cubes subject to an incident plane wave in the *z*-direction with the E field in the *y*-direction. The fields are plotted in the *yz*-plane bisecting the gap between the cubes as shown in the inset. The fields plotted are the E field with the red representing a high complex magnitude and blue representing a low complex magnitude. The arrows indicate the direction of the E field.

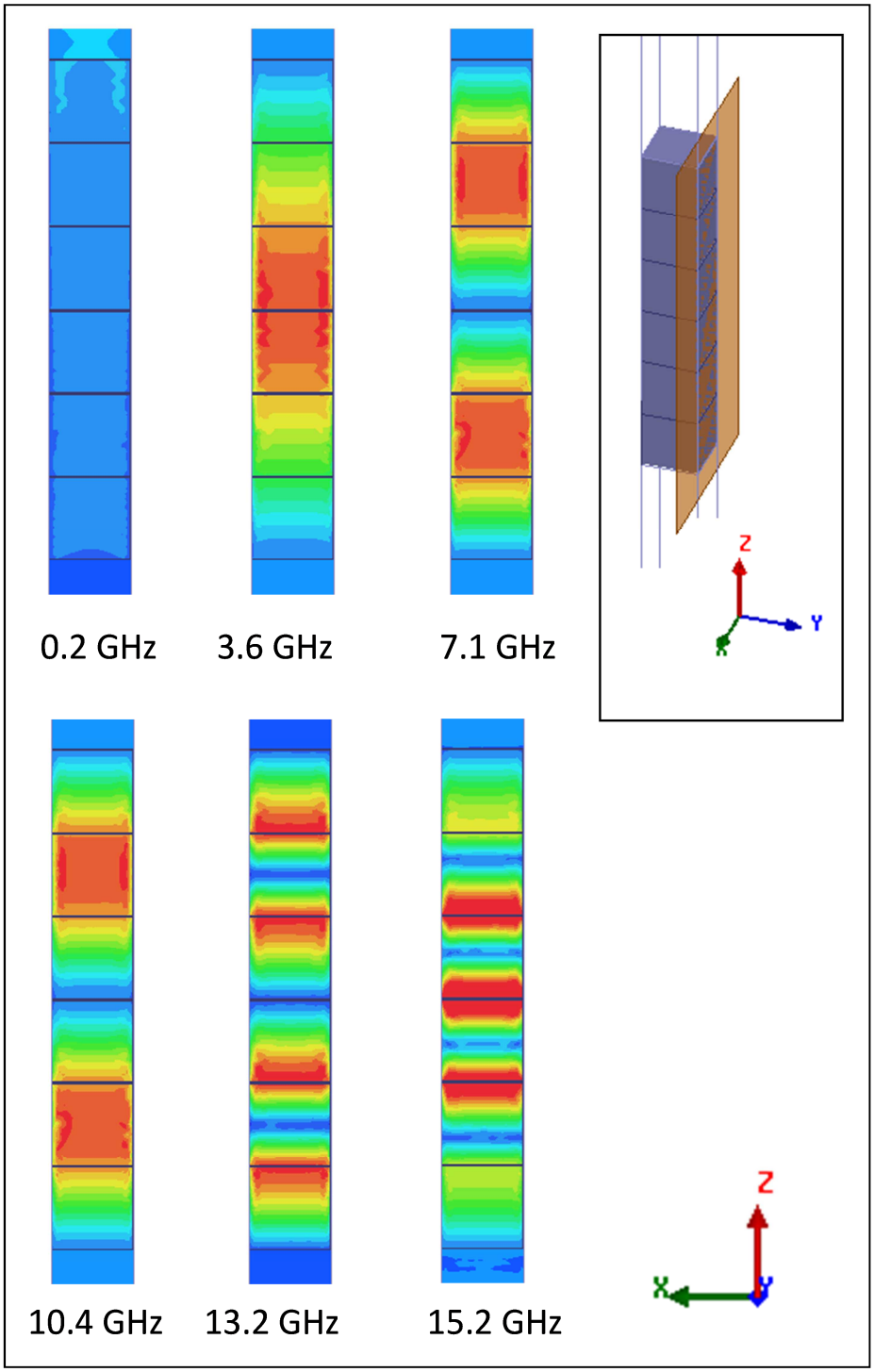

Figure 27: Magnetic field plots for an array of PEC cubes subject to an incident plane wave in the *z*-direction with the E field in the *y*-direction. The fields are plotted in the *xz*-plane bisecting the gap between the cubes as shown in the inset. The fields plotted are the H field with the red representing a high complex magnitude and blue representing a low complex magnitude.

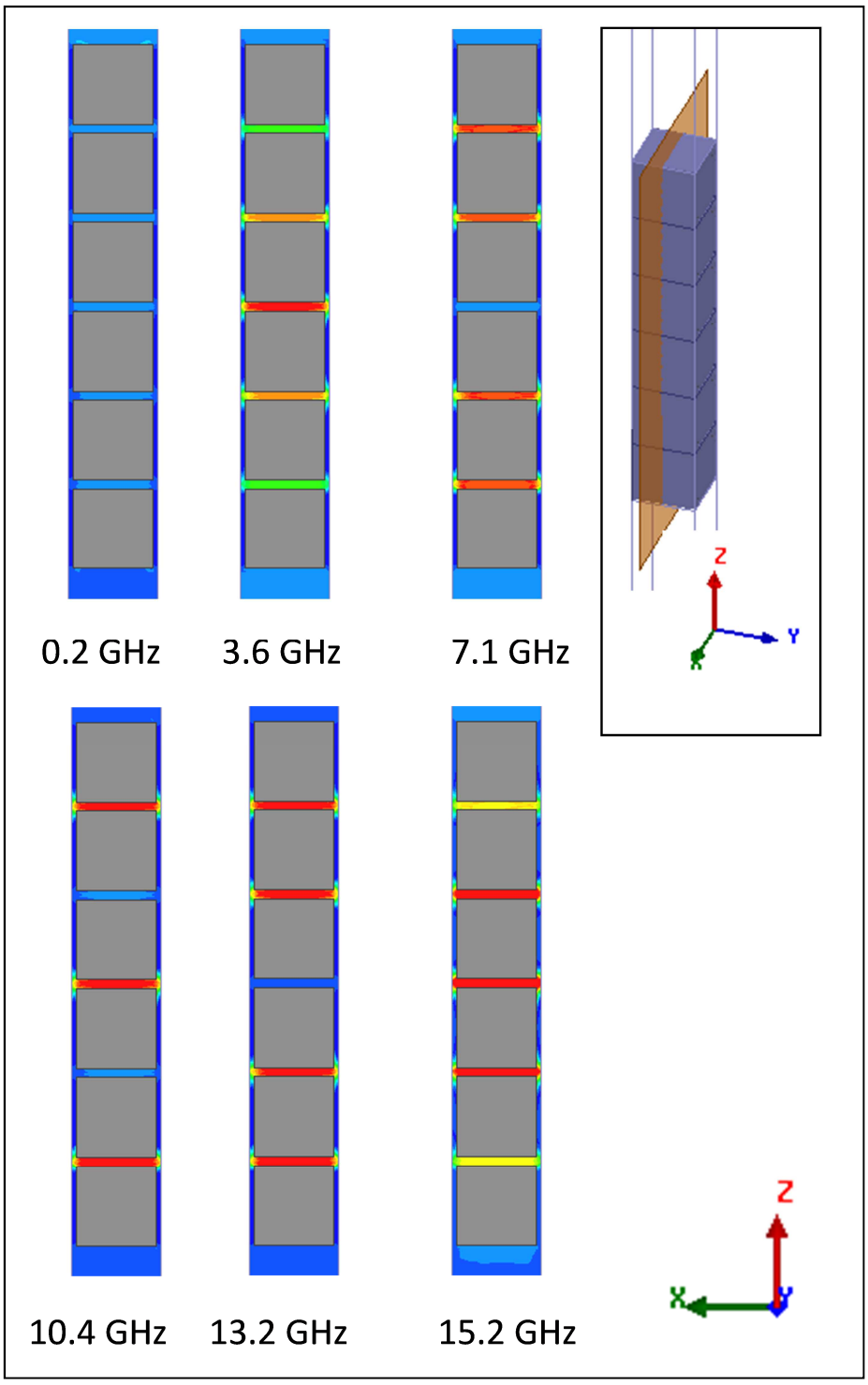

Figure 28: Magnetic field plots for an array of PEC cubes subject to an incident plane wave in the *z*-direction with the E field in the *y*-direction. The fields are plotted in the *xz*-plane bisecting the cubes as shown in the inset. The fields plotted are the H field with the red representing a high complex magnitude and blue representing a low complex magnitude.

The preliminary measurements of an array of structured elements hint at the existence of higher order bands of modes. Extending the frequency of the

modelling of the PEC cubes up to 50 GHz (Figure 29) clearly shows the existence of these higher order modes. The transmission response shows band structure with three families of modes separated by two wide band gap regions from 16 GHz to 29 GHz and from 32 GHz to 47 GHz. The response of an array structure is discretised by the number of layers in the array in the direction of propagation (in this case the z direction). The second group of modes are much more tightly spaced suggesting a very high index over a narrow frequency range. These higher order modes require further investigation, but this thesis is only concerned with the lowest band where the period of the structure is much less than the wave length and hence the structure can, for these lower frequencies, be considered a metamaterial.

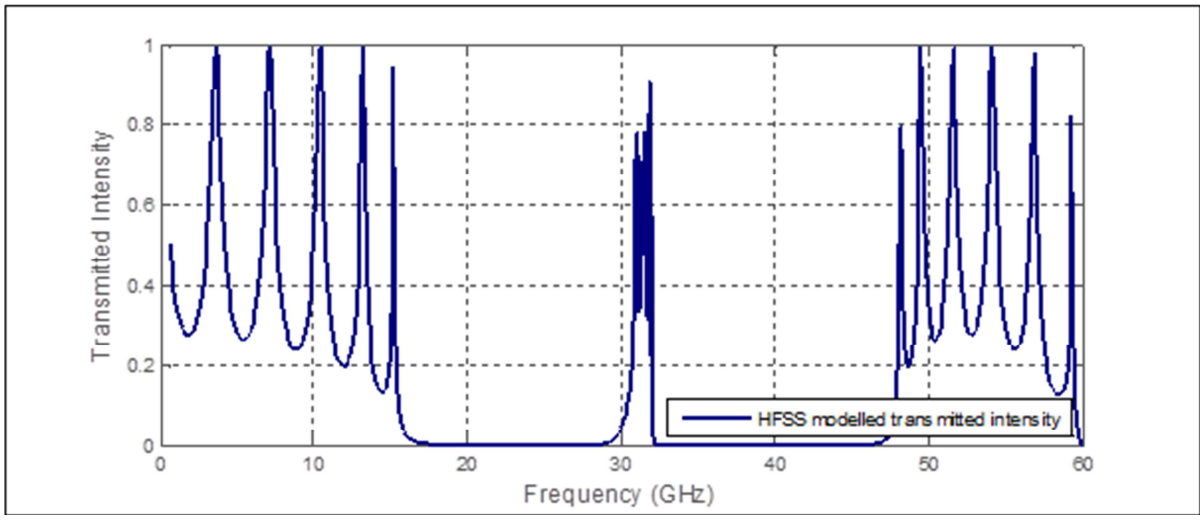

Figure 29: Plot showing the normalised transmission through a six layered array of PEC cubes.

3.2.2 Measurement of an array of Structured Elements

Sixty structured elements 4.2 mm in dimension, arranged in two (6×5×1) layers, held together with a band of low dielectric constant, and separated by small acrylic stickers were measured using the permeameter device (see Figure 20). The faces of each element had a square acrylic patch adhered to them so that when arranged into an array structure there was uniform separation. Figure 30 shows the measured frequency-dependent reflected and transmitted intensities

from 100 MHz to 8 GHz. Similarly to the solid cube measurements the modal response of the structure is evident with lower order modes present with a band gap occurring above 4.8 GHz (see Figure 30).

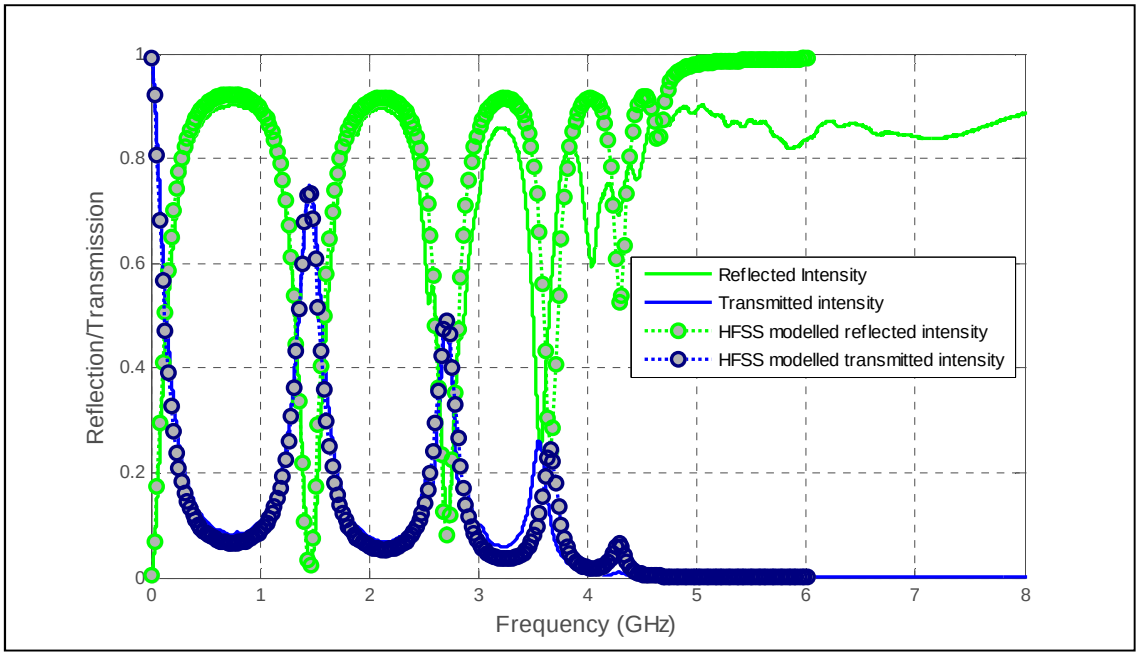

Figure 30: Measured (continuous lines) and modelled (dashed lines) reflection and transmission intensity for a six layered array of structured elements.

The EM response of the sample was modelled in HFSS with a plane wave incident having its *k*-vector in the *z* direction through an array of copper elements 4.2 mm in dimension (with an individual plate size of 2.8 mm × 2.8 mm) separated by 85 μm thick acrylic (ε = 2.55 + 0.001i). The structure was modelled as being of infinite extent in the *xy*-plane but only six elements deep in the *z*-direction and was modelled from 0.6 GHz to 6 GHz. The model fits are the dotted lines in Figure 30 which generally show good agreement. Some of the higher frequency modes are less well defined in the measured response which is likely to be due to loss within the system coupled with the tolerances in the sample manufacture which become more significant as the frequency increases and approaches the lower edge of the band gap. The model fit was achieved by modifying the value of the dielectric constant of the acrylic spacer (to ε = 2.35 + 0.001i) in the model to account for the inevitable air gap between elements present in the measured sample. It can be clearly seen that, compared with the array of solid cubes, the band-gap occurs at a lower

frequency of 4.8 GHz. This results in the frequency range over which the permittivity and permeability can be considered non-dispersive being greatly reduced compared with the array of cubes (as seen in Figure 31). The frequency range over which the structure can be considered non-dispersive is now only approximately 2 GHz.

Figure 31 shows the frequency plotted of each mode for both the measured and modelled response of an array of structured elements compared to that for an array of solid cubes. Modes are more tightly spaced in the structured element response, indicating the, as expected, increase in effective index of the structured element array. This is confirmed by the extracted permittivity and permeability values which were extracted using a fitting routine to a three layer Fresnel model as discussed in section 2.3. Figure 32 shows the measured reflection and transmission of the array of structured elements compared with that of an equivalent dielectric with a permittivity of 26 + 0.3i and a permeability of 0.56 + 0.01i resulting in an effective index of 3.9 + 0.07i. This compares with an index value of 2.25 + 0.04i for the array of solid cubes.

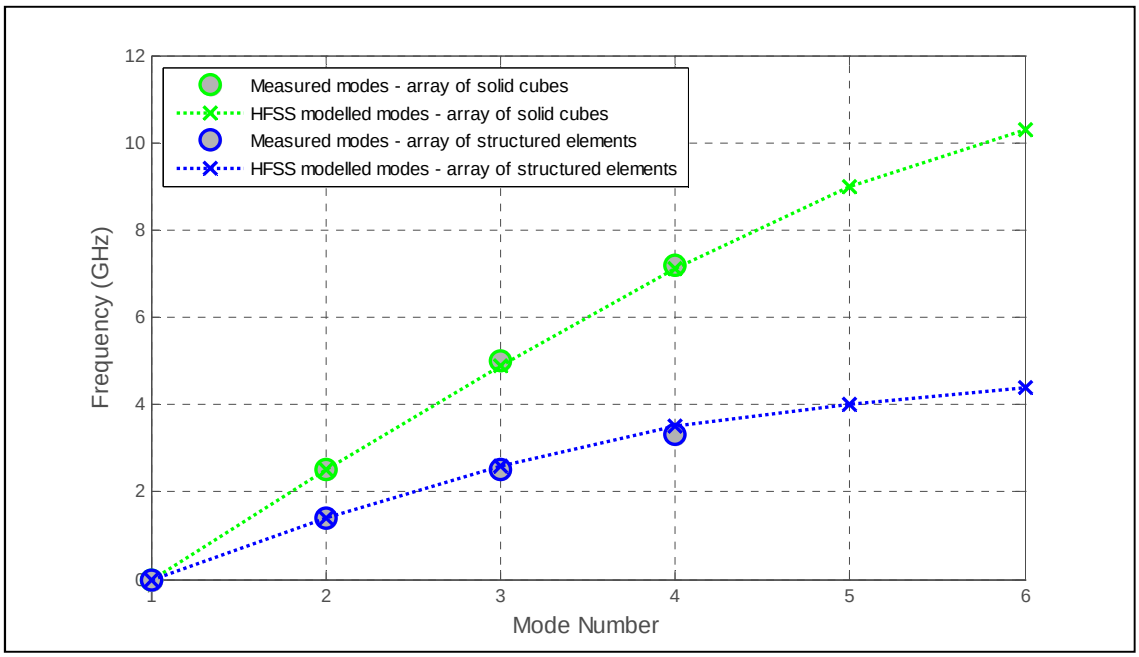

Figure 31: Comparison of modal frequencies between the response from array of cubes and an array of structured elements.

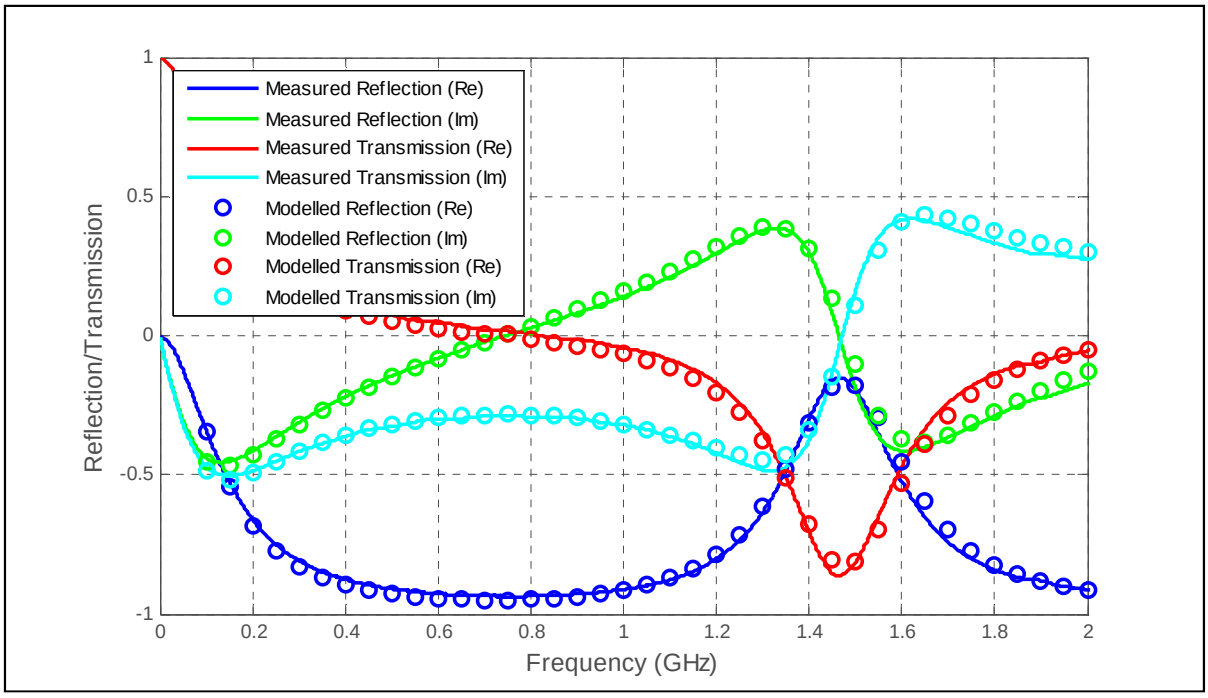

Figure 32: Comparison of the measured reflection and transmission with the modelled response of an equivalent material with ε = 26.0 + 0.29i, μ = 0.56 + 0.01i.

Compared to the solid cubes, the permittivity of the structured cubes shows a reduction in the real part from nearly 50 to 26. This can be explained as the permittivity is due to the capacitive effect between individual elements and is highly dependent on the size of the plates. Due to limitations of the fabrication technique, the plate size of the structured cubes is 2.8 mm compared to the 4.2 mm face side for the solid cubes. However, due to a reduction in the current loops the real part of permeability has increased from 0.1 to 0.56 resulting in the refractive index being nearly doubled from 2.25 to 3.91.

To further investigate the characteristics of an array of structured elements FEM modelling was carried out of an ideal structure comprising of PEC elements suspended in a vacuum. As with the array of solid cubes, an ideal structure was modelled as key characteristics (particularly at higher frequencies) are more easily observed in loss-less structures.

The FEM software models transmission and reflection of a plane wave incident with the *k*-vector in the *z* direction and the *E* field in the *y*-direction through an

array of elements of infinite extent in the *xy*-plane but only six cubes deep in the *z*-direction.

Figure 33 shows the electric field plots for a single element of an array of solid cubes and also for structured elements. In both cases the fields are plotted of the second layer of a six layered structure for the third mode (7.1 GHz for the array of cubes and 3.8 GHz for the array of structured elements). It can be seen that the electric field is concentrated between neighbouring elements and acts primarily in the y-direction normal to the face of the cube or connected plate. It is also apparent that very little of the electric field penetrates into the inner region of the structured elements.

The corresponding magnetic field plots of the third mode for an array of solid cubes and an array of structured elements (see Figure 34) show that the modal shape of the fields is similar between the two structures. It can also be seen that the magnetic field penetrates into the inner region of the structured element.

The FEM modelling has shown that the electric and magnetic fields are decomposed to different regions within the structure and in particular that the inner region of the structured element is largely shielded from the electric field but can be penetrated by the magnetic field.

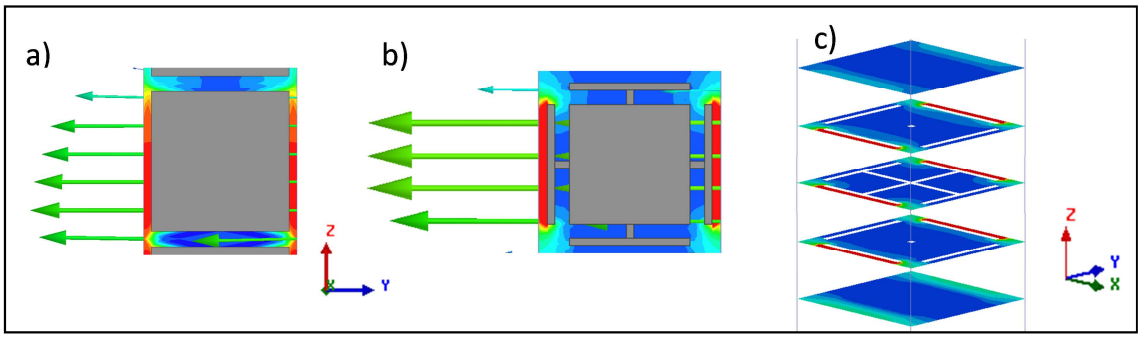

Figure 33: Electric field plots for a single element of an array of a) cubes and b) a structured elements. Fields are plotted of the second layer of a six layered structure for the third mode (7.1 GHz for the array of cubes and 3.8 GHz for the array of structured elements.) c) Shows horizontal slices through the electric field of the structured element. The fields plotted are the time averaged E field with the red representing a high magnitude and blue representing a low magnitude. The arrows indicate the direction of the E field.

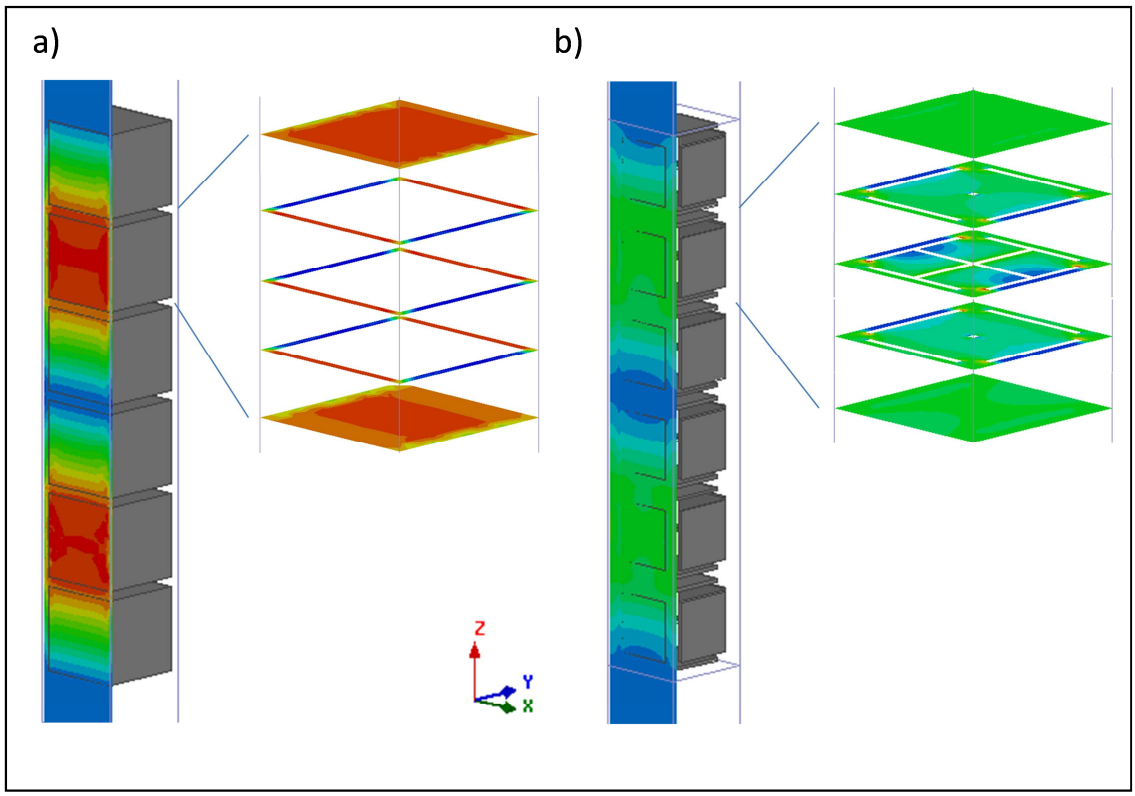

Figure 34: Magnetic field plots for a six layered array of a) cubes and b) a structured elements. Fields are plotted for the third mode (7.1 GHz for the array of cubes and 3.8 GHz for the array of structured elements). The fields plotted are the time averaged H field with the red representing a high magnitude and blue representing a low magnitude.

In conclusion, transmission measurements using a modified stripline geometry have shown that connected plate structures, forming open cubes, which maintain the capacitive effect between neighbouring elements while reducing the area of the current loops results in a metamaterial with a substantially enhanced effective refractive index. The measurements and modelling detailed in this thesis show that the connected plate structure strongly decomposes the electric and magnetic field components into different regions within the structure. This accords fully with the suggestion by Shin et al [1] that this structure gives a substantially enhanced effective index. It is apparent from this study that filling different regions of the structure with materials tailored to affect either the electric or magnetic fields will give much greater control of both the effective permittivity and permeability. This forms the basis for the further development of these structures discussed in Chapter 4.

3.3 Chapter Summary

In Chapter 3 the effects proposed by Shin et al. [1] have been experimentally verified. It has been shown that changing the structure of the elements in such a way as to reduce the current loops while maintaining the capacitive effects does indeed increase the effective index of the structure. The remainder of this thesis explores further ways in which the structure can be altered to extend the independent control over the effective electric and magnetic properties of the structure.

4 Further Independent Control of Permittivity and Permeability

In Chapter 1 it was stated that a material with a controlled positive index and a high degree of anisotropy is required for many of the applications and devices defined by transformation optics. Chapter 4 develops the structures investigated in Chapter 3, increasing the independent control of the permittivity and permeability and introduces anisotropy.

It has been confirmed experimentally that shaping the elements of an array can increase the effective index of the structure by decreasing the area of the current loops around the elements while maintaining the capacitive effect between elements. Field plots of the structure show that the electric field and magnetic field are decomposed into different regions within the structure. In Chapter 4 we exploit this field decomposition and explore via modelling two different ways of furthering the independent control over the electric and magnetic properties of the structured element array. Firstly, the structured elements consisting of six orthogonal connected plates are filled with a high permeability material in an attempt to increase the control over the magnetic properties of the structure. Secondly, the element spacing and the material properties of the spacer materials are varied to introduce anisotropy into the structure.

4.1 Filling the Structured Elements

In Chapter 3 it was shown that the electric field is confined to the gaps between the elements while the magnetic field, although concentrated in the gaps between elements also penetrates into the inner central region of the elements. The idea explored in this section is that filling the central region of the structured cubic element with high permeability material may increase the effective permeability of the structure while not significantly affecting the effective permittivity of the structure.

A FEM model constructed similar to that used in Chapter 3 consisting of a PEC elements suspended in free space was filled with materials of differing

permittivity and permeability. An individual unfilled and filled element is illustrated in Figure 35.

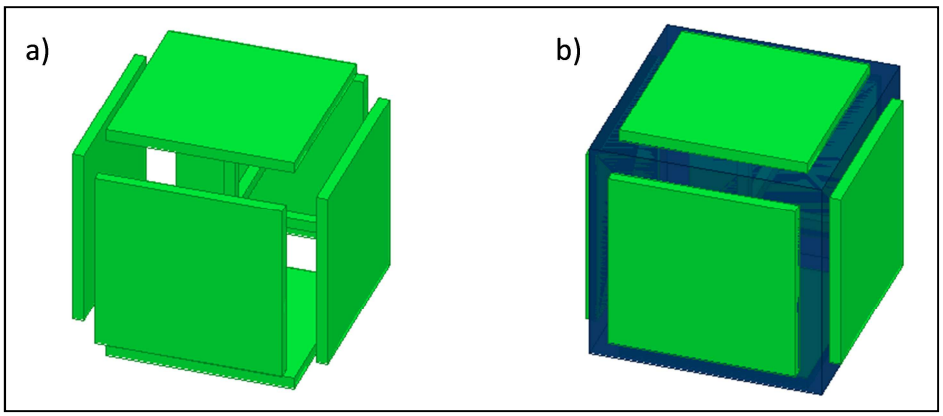

Figure 35: Diagram showing the individual a) unfilled structured elements and b) filled structured elements.

We begin by considering ideal lossless filler materials in order to investigate this concept. The HFSS software was used to model transmission and reflection of a plane wave incident with the *k* vector in the *z*-direction and the E field in the *x*-direction through an array of structured elements of infinite extent in the *xy*-plane but being only six elements deep in the *z*-direction. A six layered structure with a period of 5 mm and a cube dimension of 4.5 mm and filled with four different filler materials was modelled from 0.2 GHz to 6 GHz resulting in the frequency dependent transmission response shown in Figure 36. It can be seen that increasing the permeability of the filler materials has greater effect on the response than increasing the permittivity of the filler. At lower frequencies where the material is in the metamaterial regime, the response is dominated by the changes in permeability of the filler with the changes in filler permittivity having minimal effect. At higher frequencies where the material becomes dispersive, the difference in permittivity of the filler has a larger impact due to a greater penetration of the electric field into the inner region of the cube. Increasing the permeability results in the modes being more tightly spaced suggesting an increase in index. This increased index is confirmed by the NRW extracted effective permeability and permittivity in the frequency range between 0.2 GHz and 1 GHz, where the structure can be considered non-dispersive, as shown in Figure 37.

Increasing the permeability of the filler increases the effective permeability of the structure, while only having a minimal impact on the effective permittivity of the structure, while increasing the permittivity of the filler has a minimal effect on both the effective permittivity and permeability.

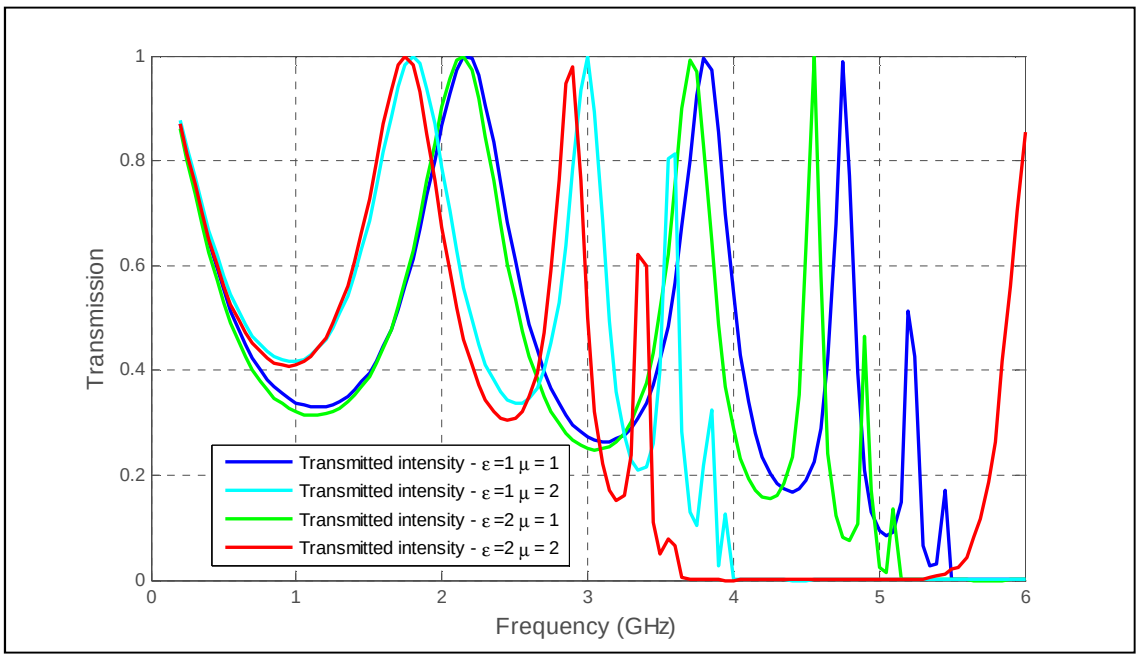

Figure 36: Plot showing the HFSS modelled transmission response for four arrays consisting of structured elements with the internal region of the elements filled with four different dielectric materials.

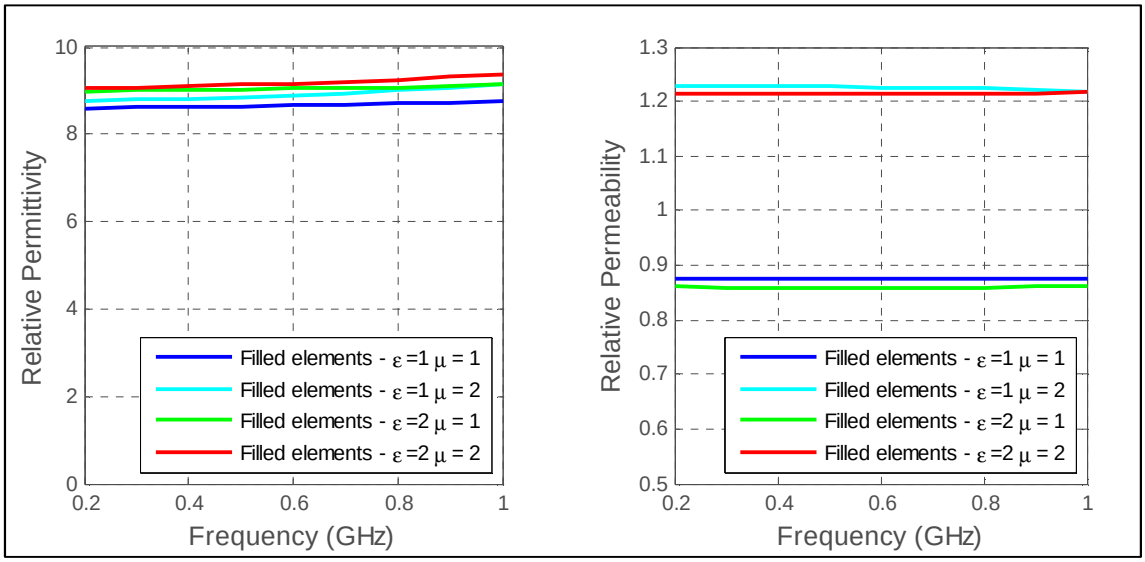

Figure 37: Plot of the extracted permittivity and permeability for four arrays consisting of structured elements with the internal region of the elements filled with four different dielectric materials.

Higher permeability filler materials were inserted into the modelled structure to explore the limitations of this permeability control.

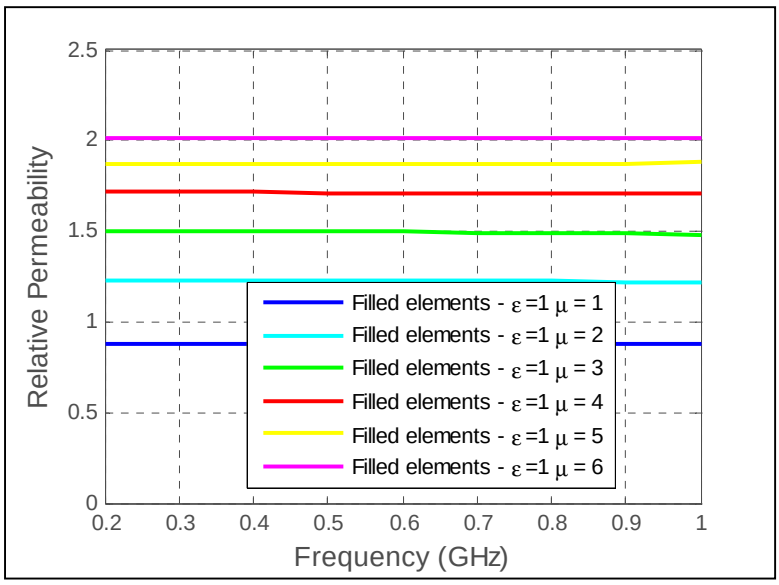

Figure 38: Plot of the extracted permeability for six array structures consisting of structured elements with the internal region of the elements filled with six different dielectric materials.

As the permeability of the filler material is increased the effective permeability of the structure increases, but appears to be approaching an upper limit. This limit is reached because the filler material is only exposed to a certain proportion of the incident magnetic field. The magnetic field in the region between the elements is not affected by the filler and this constrains the permeability to this limit.

The filler materials modelled so far in this chapter have been ideal lossless materials. We now model a more realistic filler, and Figure 39 shows the effect of adding a ferrite loaded elastomer filler ($\varepsilon = 20+0.4i$, $\mu = 4.1+0.8i$) into the structure. It should be noted that the filler material is assumed to be non-dispersive for this model. It can be seen that the addition of a filler material has increased the effective permeability of the structure from 0.75 to approximately 1.7 but the high permittivity of the filler material has also slightly increased the effective permittivity of the structure. Further work is required to investigate different filler materials and the effect of the dispersive nature of the filler material on the frequency dependence of the entire structure.

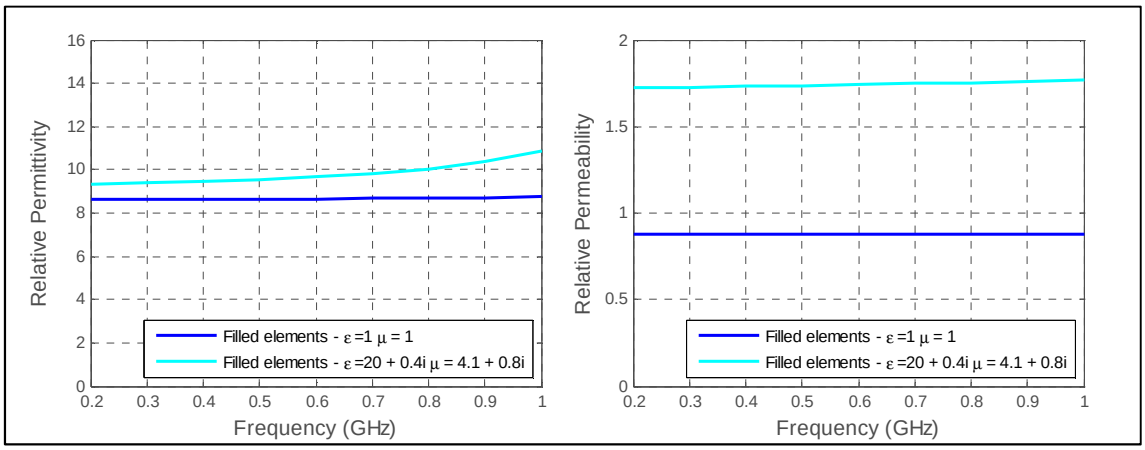

Figure 39: Plot of the extracted permittivity and permeability for two arrays consisting of structured elements with the internal region of the elements filled with free-space and a loaded dielectric material.

The initial FEM modelling detailed in this section suggests a potential to increase the control over the magnetic properties of structure by filling the inner region of the elements. There is a great deal of further work, both modelling and experimental in this area, exploring the possibilities and limitations of what can be achieved by filling such structures with dispersive filler materials.

4.2 Anisotropic Metamaterial Structures

We now investigate whether controlled anisotropy can be introduced to the metamaterial structure. Two simple mechanisms were proposed for anisotropic structures; altering the spacing between the elements and altering the material properties in the gaps between the elements as shown in Figure 40 and Figure 42.

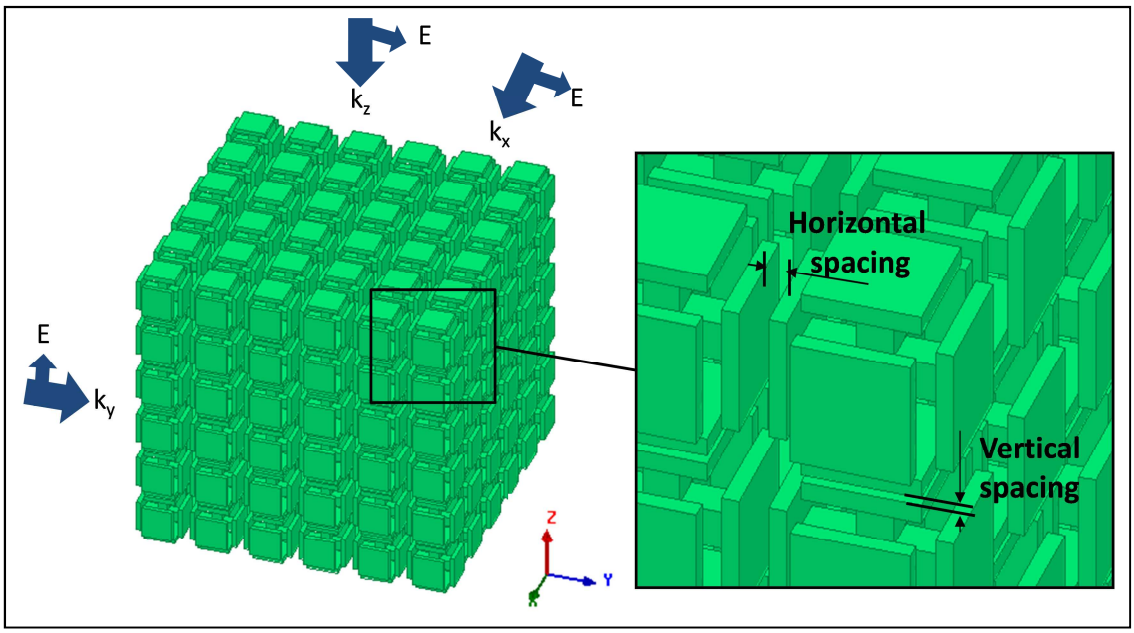

Figure 40: Diagram of anisotropic array of structured elements with a larger horizontal spacing between the elements (in the *x* and *y*-direction) and a tighter vertical spacing (in the *z*-direction). The three different directions of the propagation and polarisation are also shown.

To investigate the affect of altering the spacing between elements a FEM model was constructed similar to that used in Chapter 3 consisting of a PEC element suspended in a vacuum. The model was changed to represent propagation in three orthogonal directions through a six layered cube structure (i.e. six layers in all three directions) where the spacing between elements in the *x* and *y*-direction was set to be double that of the spacing between elements in the *z*-direction as illustrated in Figure 40.

Figure 41 show the extracted parameters for the propagation in orthogonal directions through an array with unequally spaced elements. It can be seen that the permittivity and index are different depending on the direction of propagation and polarisation with the index being 4.8 in the *x* and *z*-direction and 6.5 in the *y*-direction.

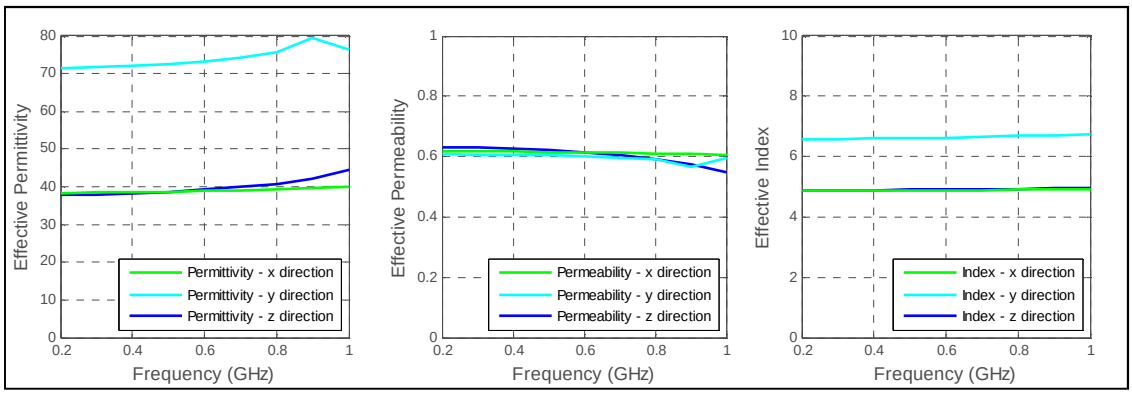

Figure 41: Plot of the extracted permittivity, permeability and index for three directions of propagation through an anisotropic structure as illustrated in Figure 40.

To investigate the affect of altering the material properties of the spacer material between elements a FEM model was constructed similar to that used in Chapter 3 consisting of a PEC element suspended in a vacuum. The model was changed to represent propagation in three orthogonal directions through a six layered cube structure (i.e. a 6×6×6 array) where the index of spacer material between elements in the *x* and *y*-direction was set to be higher than that of the spacer between elements in the *z*-direction as illustrated in Figure 42.

Figure 43 show the extracted parameters for the propagation in orthogonal direction through an array with spacers of varying material. It can be seen that the permittivity and index are different depending on the direction of propagation and polarisation with the index being 4.8 in the *x* and *z*-direction and 6 in the *y*-direction.

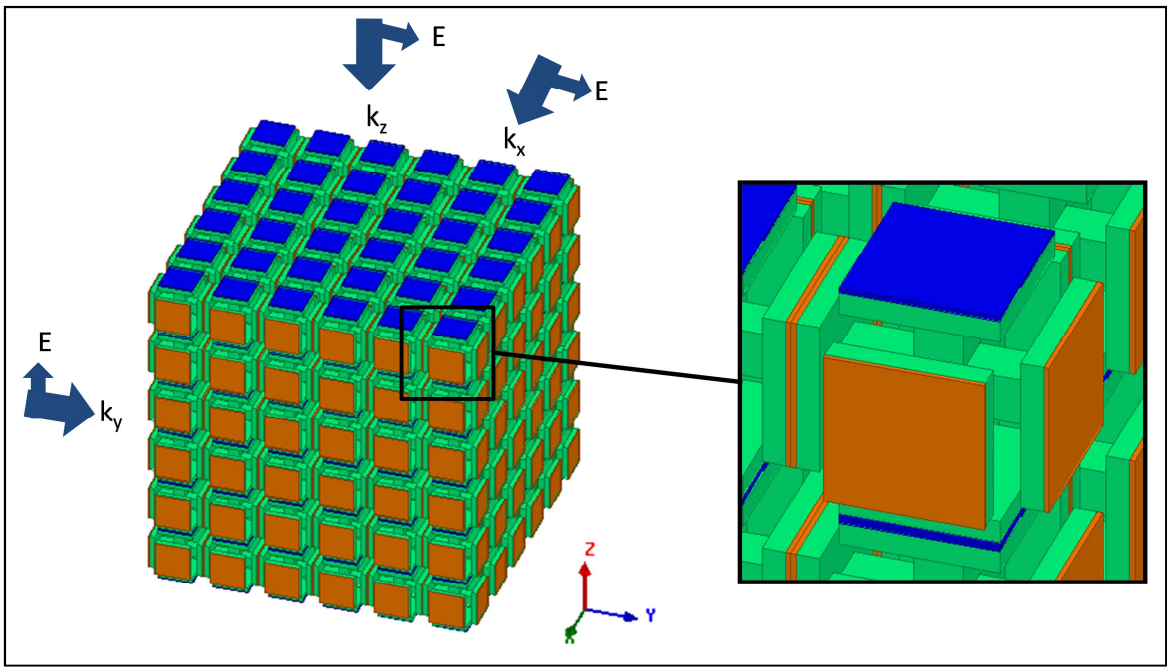

Figure 42: Diagram of anisotropic structure with a higher dielectric spacer material (blue) between layers in the *z* direction and a lower dielectric spacer material (orange) between layers in the *x* and *y*. The three different directions of the propagation and polarisation are also shown.

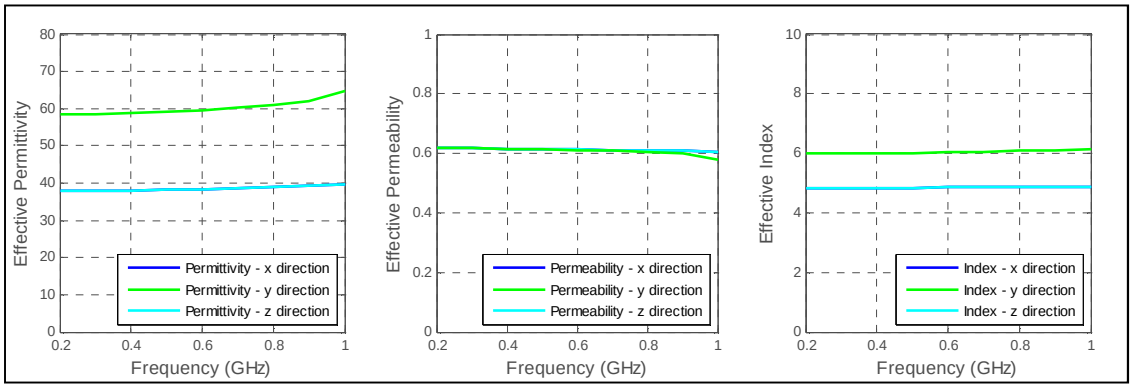

Figure 43: Plot of the extracted permittivity, permeability and refractive index for three directions of propagation through an isotropic structure as illustrated in Figure 42. It should be noted that the traces for the *x* and *z*-direction directly overlay each other.

It has been shown that anisotropy can be simply introduced into the structure by varying the spacing between elements and/or by varying the material properties of the spacer material. Much further work is required to investigate the extent, limitations and applicability of these anisotropic three dimensional metamaterials. It should also be noted that thus far it is only the permittivity that is directional; the permeability remains essentially constant in all directions through the structure. Further work could of course be undertaken changing the

character of the metal plates on different faces to create anisotropic permeability.

4.3 Chapter Summary

Chapter 4 shows that filling different regions of the structure with materials tailored to affect either the electric or magnetic fields gives a much greater control of both the effective permittivity and permeability of the structure. For some applications, particularly following transformation optics, it is desirable to have anisotropy within the structure. In this chapter it is shown that anisotropy can be introduced into the structure by varying the spacing or spacer materials between elements through the structure. The modelling work presented here establishes the concept of filling these shaped structures, originally proposed by Shin [1] for index enhancement, to gain a further level of control over the electric and magnetic properties of the structured metamaterial. Much further modelling and experimental work is required to explore what can be achieved with filled three dimensional structured metamaterials.

5 Conclusions

5.1 Summary of Thesis

The work detailed within this thesis concerns the development of 3D metamaterials with independent and controllable electric and magnetic properties over a large frequency range.

In Chapter 1, an introduction to three dimensional broadband metamaterials is presented. A brief historic overview of research in the area of metamaterials and transformation optics is provided as well as a brief review of some key developments in metallic metamaterials. Developments in metallic metamaterials including arrays of capacitive plates and three dimensional structures culminated in a structure proposed by Shin et al. [1] of a three dimensional array of cubic shaped elements consisting of six square metallic plates linked by orthogonal wires. The work of Shin et al. explores a general procedure for enhancing the permittivity by generating a large electric dipole response while maintaining permeability through the prevention of the formation of large area current loops.
In Chapter 1 the 3D metamaterial structures proposed by Shin were introduced which formed the basis of the work detailed in the remainder of this thesis.

Chapter 2 concerns the electromagnetic modelling and measurement methods used to investigate the EM characteristics of the 3D metamaterial structures. The finite element method (FEM) modelling tool HFSS was firstly introduced and then demonstrated generating the EM response of a simple array of cubes. Methods for determining the permittivity and permeability from the measured and modelled transmission and reflection response were presented and discussed. This chapter also detailed the measurement method including sample fabrication and the stripline measurement and characterisation technique.

In Chapter 3 the results proposed by Shin et al. [1] were experimentally verified. It has been shown that changing the structure of the elements in such a way as to reduce the current loops while maintaining the capacitive effects does indeed increase the effective index of the structure. The structured element arrays showed a nearly two-fold increase in refractive index from 2.1 (for the solid cubes) to 3.9. This accords fully with the suggestion by Shin et al. [1] that this structure gives a substantially enhanced effective index.

The modelling detailed in this thesis show that the connected plate structure strongly decomposes the electric and magnetic field components into different regions within the structure. In Chapter 4 the field decomposition shown in Chapter 3 was exploited and it was shown that filling different regions of the structure with materials tailored to affect either the electric or magnetic fields gives a much greater control of both the effective permittivity and permeability. This yields the possibility of designing materials with independent and spatially varying permittivity and permeability.

In Chapter 4 it was also shown that anisotropy can be introduced into the structure by varying the spacing or spacer material between elements through the structure. The modelling work presented established the concept of filling these shaped structures (originally proposed by Shin [1] for index enhancement) to gain a further level of control over the electric and magnetic properties of the structured metamaterial. Much further modelling and experimental work is required to explore what can be achieved with filled three dimensional structured metamaterials.

5.2 Future Work

The area of three-dimensional metamaterials is reasonably immature, with a vast range of applications resulting in a huge list of potentially interesting future work from which a small selection of ideas is presented here.

In Chapter 4 filling the regions of the structure and varying the spacing between elements was explored in order to achieve a greater control of the electric and magnetic properties while also having the potential to introduce anisotropy into

the structure. This work should be extended through both electromagnetic modelling and experiment to fully explore the limitations and possibilities of this approach. Filling the structure with real high permeability materials could give even greater index enhancement or could be used to improve the impedance match of the material. Anisotropic structures could also be further investigated exploring the limitations of varying element spacing and spacer materials as well as investigating varying the aspect ratio of the individual elements.

Other areas of future work include extension to the electromagnetic modelling in Chapter 3 (Figure 29) where the material can no longer be considered as a metamaterial as at higher frequencies the wavelength is no longer much shorter than the period of the structure. However the modal response of the structure may warrant further investigation as the response of the structure may give the equivalent response to that of an ultrahigh index material albeit over a limited frequency band.

Another development would be to investigate different array structures such as a tetrahedral array consisting of four triangular plates connected by four wires meeting in the centre of the element. Validation would be required that such a structure works in the same way as the array of structured cubic elements, maintaining the capacitive effect between elements while reducing the diamagnetic effects associated with the current loops around the elements. Grading the properties of the structure and controlling any introduced anisotropy may be challenging, but a tetrahedral structure would provide more flexibility for applications where it is beneficial to have more complicated non-planar geometries.

Significant issue with experimentally investigating the developments of 3D structures and eventual realisation for a practical application is the fabrication of the complex 3D structures. Advances in technologies such as multi-material advanced layer manufacture (ALM) and direct write will make it easier to realise complex periodic structures constructed from metallic and dielectric materials. Advances in these and other technologies will allow the miniaturisation of such structures and would extend the frequency range for which they could operate.

6 References

[1] J. Shin, J. Shen and S. Fan, “Three-dimentional metamaterials with an ultrahigh refractive index,” *Phys. Rev. Lett.,* vol. 102, p. 093903, 2009.

[2] J. B. Pendry, D. Schurig and D. R. Smith, “Controlling electromagnetic fields,” *Science,* vol. 312, pp. 1780-1782, 2006.

[3] U. Leonhardt, “Optical Conformal Mapping,” *Science,* vol. 312, pp. 1777-1780, 2006.

[4] M. Rahm, S. Cummer, D. Schurig, J. B. Pendry and D. R. Smith, “Optical Design of Reflectionless Complex Media by Finite Embedded Coordinate Transformation,” *Phys.l Rev. Lett.,* vol. 100, p. 063903, 2008.

[5] Y. Lai, H. Chen, Z. Zhang and C. Chan, “Complementary media invisibility cloak that cloaks objects at a distance outside the cloaking shell,” *Phys. Rev. Lett.,* vol. 102, p. 093901, 2009.

[6] J. Li and J. B. Pendry, “Hiding under the carpet: A new strategy for cloaking,” *Phys. Rev. Lett.,* vol. 101, p. 203901, 2008.

[7] R. Yang, W. Tang, Y. Hao and I. Youngs, “A Coordinate Transformation-Based Broadband Flat Lens via Microstrip Array,” *IEEE Antennas and Wireless Propag. Lett.,* vol. 10, pp. 99-101, 2011.

[8] P. Tichit, S. Burokur and A. Lustrac, “Ultradirective antenna via transformation optics,” *J. App. Phys.,* vol. 105, p. 104912, 2009.

[9] J. T. Turpin, Z. Jiang, D.-H. Kwon, P. L. Werner and D. H. Werner, “Metamaterial-Enabled Transformation Optics Lenses for Antenna Applications,” in *Antennas and Propagation (EuCAP), 2010 Proceedings of the Fourth European Conference*, 2010.

[10] J. C. Bose, “On the rotation of plane of polarisation of electric waves by a twisted structure,” *Proc. Roy. Soc.,* vol. 63, pp. 146-152, 1898.

[11] I. V. Lindell, A. H. Sihvola and J. Kurkijarvi, “The last Hertzian, and a Harbinger of electromagnetic chirality,” *IEEE Antenna Propag. Mag.,* vol. 34, pp. 24-30, 1992.

[12] W. E. Kock, “Metallic delay lenses,” *Bell Sys. Tech. J.,* vol. 27, pp. 58-82, 1948.

[13] V. G. Vesalago, “ The Elecrodynamics of Substances with Simultaneously Negative Values

of ε and μ," *Sov. Phys. Uspekhi,* vol. 10, pp. 509-514, 1967.

[14] J. B. Pendry, A. J. Holden, D. J. Robbins and W. J. Stewart, "Magnetism from Conductors,and Enhanced Non-Linear Phenomena," *IEEE Trans. Microwave Theory and Techniques,* vol. 47, pp. 2075-2084, 1999.

[15] D. R. Smith, W. J. Padilla, D. C. Vier, S. C. Nemat-Nasser and S. Schultz, "Composite Medium with Simultaneously Negative Permeability and Permittivity," *Phys. Rev. Lett.,* vol. 84, p. 4184, 2000.

[16] R. A. Shelby , D. R. Smith and S. Schultz, "Experimental verification of a negative index of refraction," *Science,* vol. 292, p. 77, 2001.

[17] D. Sievenpiper, L. Zhang and E. Yablonovitch, "High-Impedance Electromagnetic Ground Planes," *Microwave Symposium Digest, 1999 IEEE MTT-S International,* vol. 4, pp. 1529 - 1532, 1999.

[18] D. Sievenpiper, High-impedance electromagnetic surfaces, Ph.D. dissertation, Department of Electrical Engineering, University of California, Los Angeles, CA, 1999.

[19] S. Gu, J. P. Barrett, T. H. Hand, B. -I. Popa and S. A. Cummer, "A broadband low-reflection metamaterial absorber," *J. App. Phys.,* vol. 108, p. 064913, 2010.

[20] L. K. Sun, H. F. Cheng, Y. J. Zhou and J. Wang, "Broadband metamaterial absorber based on coupling resistive frequency selective surface," *Optics Express,* vol. 20, no. 4, pp. 4675-4680, 2012.

[21] A. P. Feresidis, G. Goussetis, S. Wang and J. C. Vardaxoglou, "Artificial Magnetic Conductor Surfaces and Their Application to Low-Profile High-Gain Planar Antennas," *IEEE Trans. Antennas and Propag.,* vol. 53, pp. 209 - 215, 2005.

[22] Y. Zhang, J. Hagen, M. Younis, C. Fisher and W. Wiesbeck, "Planar artificial magnetic conductors and patch antennas," *Special Issue on Metamaterials, IEEE Trans. Antennas Propag.,* vol. 51, p. 2704–2712, 2003.

[23] J. Shen, P. B. Catrysse and S. Fan, "Mechanism for Designing Metallic Metamaterials with a High Index of Refraction," *Phys. Rev. Lett.,* vol. 197401, 2005.

[24] B. Wood and J. B. Pendry, "Metamaterials at zero frequency," *J. Phys.: Condens. Matt.,* vol. 19, p. 076208, 2007.

[25] D. F. Sievenpiper, "*3D Metallo-Dielectric Photonic Crystals with Strong Capacitive Coupling between Metallic Islands," Phys. Rev. Lett.,* vol. 80 pp. 2829-2832, 1998.

[26] M. Choi, S. H. Lee, Y. Kim, S. B. Kang, J. Shin, M. H. Kwak, K.-Y. Kang, Y.-H. Lee, N. Park and B. Min, “Transmission through stacked 2D periodic distributions of square conducting patches,” *Nature,* vol. 470, p. 369, 2011.

[27] M. Qiu, M. Yan, J. Hao, W. Yan and J. Wang, “Tranformational Optics for designing superlenses,” *Electromagnetics in Advanced Applications, 2009. ICEAA '09. International Conference on pp. 944-947*, 2009.

[28] R. Liu, C. Ji, J. Mock, J. Chin, T. Cui and D. Smith, “Broadband Ground-Plane Cloaking,” *Science,* pp. 366-369, 2009.

[29] U. Leonhardt and T. Tyc, “Broadband Invisability by Non-Euclidean Cloaking,” *Science,* pp. 110-112, 2009.

[30] S. M. Mansfield and G. S. Kino, “Solid Immersion Microscope,” *App. Phys. Lett.,* vol. 57, p. 2615.

[31] J. Yook and L. P. Katehi, “Micromachined Patch attenna With Controlled Mutual Coupling Surface Waves,” *IEEE Trans. Antennas and Propag.,* vol. 49, 2001.

[32] Ansoft, “HFSS Computational Software”.

[33] A. M. Nicholson and G. F. Ross, “Measurement of the intrinsic properties of Materials by Time Domain Techniques,” *IEEE Trans. Instrum. Meas.,* vol. 19, pp. 377-382, 1970.

[34] W. B. Weir, “Automatic Measurement of Complex Dielectric Constant and Permeability at Microwave Frequencies,” *Proceedings of the IEEE,* vol. 62, pp. 33-36, 1974.

[35] J. Baker-Jarvis, E. J. Vanzura and W. M. Kissick, “Improved technique for determining complex permittivity with the transmission/reflection method.,” *IEEE Trans. Microwave Theory,* vol. 38, p. 1096, 1990.

[36] Z. Abbas, R. D. Pollard and R. W. Kelsall, “Complex Permittivity Measurements at Ka-band using rectangular dielectric waveguide,” *IEEE Trans. Instrum. Meas.,* vol. 50, p. 1334, 2001.

[37] D. M. Pozar, “Transmission Lines and Waveguides,” in *Microwave Engineering*, John Wiley & Sons, Inc., 2005, pp. 91-160.

[38] W. Barry, “A Broad-Band, Automated, Stripline Technique for the Simultaneous Measurement of Complex Permittivity and Permeability,” *IEEE Trans. Microwave Theory,* vol. 34, p. 80, 1986.